Chapter 4
Effective Field Theories of Loosely Bound Nuclei

U. van Kolck

4.1 Introduction

Exotic nuclei challenge models constructed for ordinary nuclei, which differ in their predictions for the positions of the driplines. Near these borders of the nuclear chart, a nucleus has one or more loosely bound nucleons that can easily be separated from the rest. In the simplest "halo" or "cluster" configurations, one or more clusters of tightly bound nucleons ("cores") are surrounded by a few nucleons at relatively large distances, which exceed the range of the strong force, $r_0 \sim \hbar/m_\pi c \simeq 1.4$ fm where $m_\pi \simeq 140\,\mathrm{MeV}/c^2$ is the pion mass. Since in classical mechanics the orbital distance is given by the range of the force, these loosely bound systems are intrinsically quantum mechanical and can display a variety of peculiar phenomena. For example, in a "Borromean" halo, the system is bound even though its subsystems are not.

Nevertheless, loosely bound systems are theoretically simpler than their more deeply bound counterparts. The reason is a fundamental "decoupling" principle according to which physics at a given distance scale is insensitive to the *details* of dynamics at much shorter distances. The short-distance dynamics can be captured instead by a finite number of parameters, whose number depends on the precision we want to achieve at the scale of interest. For the large distances characteristic of loosely bound systems, we can take the potential among constituents to be, in a first approximation, Dirac delta functions. Such a simplification means that systems with different constituents, say nucleons or atoms, can have very similar dynamics, differing only in the strength of the delta functions and the relative importance of the various possible interactions. This "universality" means that one can explain phenomena across subfields of physics using the same theoretical concepts and tools.

U. van Kolck (✉)
Institut de Physique Nucléaire, CNRS/IN2P3, Université Paris Sud, 91406 Orsay, France
e-mail: vankolck@ipno.in2p3.fr

U. van Kolck
Department of Physics, University of Arizona, Tucson, AZ 85721, USA
e-mail: vankolck@physics.arizona.edu

C. Scheidenberger, M. Pfützner (eds.), *The Euroschool on Exotic Beams, Vol. IV*,
Lecture Notes in Physics 879, DOI 10.1007/978-3-642-45141-6_4,

The decoupling principle has underlaid physics research from its beginning, and for the last thirty years or so has been formalized in the concept of effective field theories (EFTs). EFTs provide a systematic method to account for short-range dynamics even when the latter is unknown. As such, this principle can be, and of course has been, applied much more widely than the exotic nuclei of interest in this school. Even in nuclear physics, its first applications, started some twenty years ago, have been to distances scales of order r_0 [1–10]. We know that the theory of strong interactions at distances small compared to $\hbar/M_{QCD}c$, where $M_{QCD} \sim 1$ GeV/c^2 is the hadronic mass scale, is given by quantum chromodynamics (QCD), a gauge theory of quarks and gluons. At larger distances QCD is non-perturbative in its coupling constant and more easily described in terms of hadrons. An EFT—"Chiral" (or "Pionful") EFT—can be constructed at distances comparable to r_0 which includes pions and correctly incorporates the approximate symmetries of QCD such as chiral symmetry. This EFT forms the basis for a description of all nuclei, and is now the main input to the rapidly developing "*ab initio*" methods for the derivation of nuclear structure and reactions.

For distances much larger than r_0, pion exchange can be regarded as a short-range effect, and nuclear interactions reduce to delta functions and their derivatives. This "Contact" (or "Pionless") EFT is relevant for light nuclei because the two-nucleon scattering lengths—that is, the two-nucleon scattering amplitude at zero energy—are much larger than r_0, for reasons that are not well understood but we will return to. Large scattering lengths signal loosely bound states, and indeed the low-energy behavior of the lightest nuclei can be described systematically in this EFT. Universality means that with relatively small modifications this EFT can be applied to atomic systems with scattering lengths that are large compared to the Van der Waals length scale. It also means that a similar EFT—"Halo/Cluster" EFT—can be constructed for larger loosely bound nuclei, where cores are treated on the same footing as valence nucleons.

These lectures are an introduction to both the general ideas behind EFTs and the specific applications to nuclear physics. The first lecture presents the ingredients of an EFT, articulates the view of the world afforded by EFTs, and gives both classical and quantum-mechanical examples. The second lecture introduces the Chiral EFT relevant for ordinary nuclei, and describes some of its features with an emphasis on the crucial, singular character of pion exchange. In the final lecture I come to the EFTs most relevant for loosely bound systems, Pionless and Halo/Cluster EFTs. These lectures are not meant as a comprehensive review of the field, for which I refer you to, for example, Refs. [11–16]. Instead, they stress basic ideas and some of the conceptual subtleties and open problems, which are often shoved under the technical rug weaved by the many successful applications of nuclear EFTs.

4.2 Nuclear Physics Scales and Effective Field Theories

Nuclear physics has a long and venerable history. A large amount of nuclear data can be described within a picture that emerged in large part before QCD:

- nuclei are essentially made out of non-relativistic nucleons with two isospin states (protons and neutrons) of nearly equal mass $m_N \simeq 940$ MeV, which interact via a potential;
- the potential is mostly two-body, with an important one-pion-exchange component, but there is evidence for smaller three-body forces;
- isospin is a good symmetry, except for electromagnetic interactions, a sizable breaking in the two-nucleon scattering lengths, and other, smaller effects—for example, the neutron-proton mass difference is just $m_n - m_p \simeq 1.3$ MeV;
- external probes, such as photons, interact mainly with each nucleon separately, although there is evidence for smaller few-nucleon currents.

In contrast, QCD with the lightest quarks has almost opposite features:

- up and down quarks have an average ("current") mass $\bar{m} = (m_u + m_d)/2$ that is relatively small, so that they can easily be relativistic, and interact via (relativistic) gluon exchange;
- the interaction is a multi-gluon, and thus multi-quark, effect;
- isospin symmetry is not obvious since the relative mass splitting $\varepsilon = (m_d - m_u)/2\bar{m} \sim 1/3$ is not particularly small;
- external probes can interact with the collective of quarks called a hadron.

This situation automatically begs a question that is now central to the field: how does nuclear structure emerge from QCD? This is a contemporary version of a problem that has defied legions of researchers for decades: what holds the nucleus together?

In these lectures we will see how EFTs help us answer this question. The key to start tackling this problem lies on its multi-scale character. If you go through the tables of the Particle Data Book [17] you will see that hadron masses cluster—with a few notable exceptions to which we will come back in the next lecture—in the few-GeV region. This observation suggests that QCD has an intrinsic mass scale $M_{QCD} \sim 1000$ MeV/c^2. On the other hand, when you put A nucleons together to form nuclei, you find, very roughly, binding energies per nucleon $B/A \sim 10$ MeV and charge radii $\langle r^2 \rangle_{ch}^{1/2}/A^{1/3} \sim 1$ fm. This is consistent with a non-relativistic dispersion relation where the typical binding momentum is $M_{nuc}c \sim 100$ MeV/c. Thus, we face three energy scales,

$$\begin{aligned} &M_{QCD}c^2 \sim m_N c^2 \simeq 1000 \text{ MeV}, \qquad M_{nuc}c^2 \sim 100 \text{ MeV}, \\ &M_{nuc}^2 c^2 / M_{QCD} \sim 10 \text{ MeV}. \end{aligned} \tag{4.1}$$

There is, of course, a very familiar multi-scale problem: the H atom, or more generally, a two-body Coulombic state with reduced mass μ. The Hamiltonian can be written in the center-of-mass frame with relative coordinate r and momentum p as

$$H = \left(\frac{p^2}{2\mu} - \frac{\alpha \hbar c}{r} \right) \left[1 + \mathcal{O}\left(\alpha; \frac{p^2}{\mu^2 c^2}; \frac{\hbar^2}{\mu^2 c^2 r^2} \right) \right], \tag{4.2}$$

where $\alpha \equiv e^2/4\pi\hbar c \simeq 1/137 \ll 1$ is the small fine-structure constant. A quick and dirty way to uncover the scales of the resulting quantum-mechanical states is to say

that they are characterized by a size $r \sim r_{at}$ and a momentum $p \sim p_{at} \sim \hbar/r_{at}$, so that the energy $E \sim \hbar^2/(2\mu r_{at}^2) - \alpha\hbar c/r_{at}$, has a minimum at $r_{at} = \hbar/(\alpha\mu c)$. There are thus three energy scales, which for the H atom are

$$\begin{aligned} &\mu c^2 \simeq m_e c^2 \simeq 0.5 \text{ MeV}, \qquad p_{at} c \sim \alpha\mu c^2 \simeq 3.6 \text{ keV}, \\ &p_{at}^2/(2\mu) \sim \alpha^2 \mu c^2/2 \sim 13.6 \text{ eV}, \end{aligned} \tag{4.3}$$

where m_e is the electron mass. As this very simple analysis shows, the three separate scales arise from the smallness of α, which also allows a controlled exploration of the effects of the corrections in Eq. (4.2).

In low-energy QCD, however, there is no obvious small coupling constant. In contrast to α, which increases (albeit slowly) as the energy scale increases, the analogous QCD fine-structure constant α_s increases as the energy scale decreases, and it becomes of $\mathcal{O}(1)$ around $M_{QCD}c^2$. Hadronic models of low-energy data have also failed to unveil any small coupling constant. So, for a controlled approach to nuclear physics we need a method to deal with multi-scale problems that does not rely on small coupling constants. Such a method is EFT.

4.2.1 Basic Ideas

An EFT is from the outset designed to address physics at the desired resolution scale, and it substitutes a small ratio of physical scales for a coupling constant as an expansion parameter. The framework evolved from the work of Weinberg, Wilson, and many others in the 60s and 70s, and was clearly articulated at the end of the 70s [18]. For a sample of introductions to EFT, see Refs. [19–22].

An EFT puts together in a single formal framework four basic ingredients, a couple of which are frequently used separately in model building:

1. **Relevant degrees of freedom.** The degrees of freedom one should use depend on the resolution we aim for. Although physics is independent of the specific choice of coordinates, some choices simplify the theoretical description significantly. Take, for example, a painting by the French Neo-Impressionist master, Georges-Pierre Seurat. Looking closely, you see that it is made of colorful blobs of paint. Yet, at the resolution scale relevant for viewing in, say, a museum, the blobs fuse together in larger-scale images, *e.g.* a face. Although we can describe any part of the painting by giving a list of blob coordinates, the same part of the painting might be more efficiently described by concepts appropriate to the scale of the larger image, *e.g.* a mustache. In other words, *choose the degrees of freedom that best fit your problem.*
2. **All possible interactions.** The effective degrees of freedom interact in all possible ways. Take another example: a system consisting of a satellite around the Earth, and the nearby Moon. Certainly, there are gravitational interactions between any two bodies of this three-body system. But there is also an indirect

effect of the Moon on the satellite motion because of the tidal deformation of the Earth. On the large distance scale set by the Earth-Moon separation ($\simeq$384 Mm), the radii of Earth ($\simeq$6.4 Mm) and Moon ($\simeq$1.7 Mm) are small and they can be well approximated by points where the whole mass of the body is concentrated. In the point-like picture, the tide-mediated interaction is represented by a three-body force, which is an effect among three bodies that disappears when any of the bodies is removed. More generally, *whatever is not forbidden is compulsory*, and exists at some level of precision.

3. **Symmetries.** Symmetries play a fundamental role in physics, which is stressed in a traditional joke. There are several versions, but they all involve a cow with deficient milk production, two other scientists (typically a biologist and a chemist) who view the problem as complex, and a physicist who thinks it simple. The physicist's solution starts with "First, consider a spherical cow…". The reason this joke is well known is that it does capture what we do. In this case, if you consider two vectors ($\mathbf{u}$, $\mathbf{v}$) used in the description of the cow, spherical symmetry will ensure that a bilinear combination of them appears in scalar quantities in the form of the scalar product ($\mathbf{u} \cdot \mathbf{v}$) rather than the most general combination of components (*e.g.* $u_1 v_2$). The lesson is that, thanks to symmetries, *not everything is allowed*. Of course, most of the time symmetries are only approximate, and indeed the joke often continues, "Next, we treat the head in perturbation theory…". That is, the other bilinear combinations do appear, but as long as the cow is pretty healthy, they are preceded by dimensionless parameters which are small compared to 1, and thus amenable to perturbation theory.
4. **Naturalness.** This is perhaps the most distinguishing feature of EFTs, adapted from a principle proposed by 't Hooft [23]. After relevant scales have been identified, the remaining, dimensionless parameters are $\mathcal{O}(1)$, unless suppressed by a symmetry. (Recall the cow non-sphericity.) The justification is Occam's razor: this is the simplest assumption one can make about an infinite number of interaction strengths. It is crucial for an EFT, because in the absence of large quantities, we can expect observables to be amenable to *an expansion in the small ratio between the scale characteristic of short-range physics left out of the theory and the distances of interest*—or, alternatively, the inverse of the corresponding momentum or energy scales. This assumption is, of course, to be revised when necessary. If interactions strengths are found to deviate systematically from it, it is possible that a particular scale has been left out or misidentified; after we account for it, naturalness is expected once again. Of course we might expect deviations for a finite number of interaction strengths anyway, in which case we speak of *fine-tuning* and incorporate it in a case-by-case basis.

Let me consider a simple classical example: a light object of mass m near the surface of a very large body that produces a gravitational acceleration of magnitude g. Simple experiments at energies $E \sim mgh$, where h is the height of the object, suggest that the important degree of freedom is the position, and that there is an (approximate) translation symmetry, so that the effective potential V_{eff} is a function of h only. This description will break down at some energy, which I will call $E_{und} \equiv$

mgR. For $E \ll E_{und}$, or equivalently $h \ll R$, the most general effective potential can be written as an expansion

$$V_{\mathit{eff}}(h) = m \sum_{i=0}^{\infty} g_i h^i = \text{const} + mgh(1 + \eta h + \cdots), \tag{4.4}$$

where g_i are parameters ($g_1 \equiv g$, $g_2 \equiv \eta g$) and I am neglecting quantum corrections that could give rise to non-analytic h dependence. Naturalness means

$$\frac{m g_{i+1} h^{i+1}}{m g_i h^i} = \frac{E}{E_{und}} \times \mathcal{O}(1) = \frac{h}{R} \times \mathcal{O}(1), \tag{4.5}$$

which in turn implies

$$g_{i+1} = \mathcal{O}\left(\frac{g}{R^i}\right). \tag{4.6}$$

If we carry out very precise experiments we can obtain values not only for g but also for η and other parameters, testing Eq. (4.6). In fact, given a desired accuracy, we need only a few terms in this expansion—in daily life only the linear one. Of course this example is somewhat artificial because we already know, thanks to Newton's apple, that, if the large object has mass M and is approximately spherical with a radius R, it produces a gravitational potential energy

$$V = -m\frac{GM}{R+h} = m\frac{GM}{R^2} \sum_{i=0}^{\infty} \left(\frac{-1}{R}\right)^{i-1} h^i. \tag{4.7}$$

In this case

$$g_{i+1} = (-1)^i \frac{g}{R^i}, \quad g = \frac{GM}{R^2}, \tag{4.8}$$

so that Eq. (4.6) is indeed fulfilled, and we can identify the breakdown scale R of the effective theory with the radius of the large body. Still, this simple example illustrates why naturalness is such a, well, natural assumption: it is not so easy to come up with situations where Eq. (4.6) would fail. If, say, we had misidentified the scale R by a factor of $\mathcal{O}(1)$, Eqs. (4.4) and (4.6) would still apply. Of course, in a more realistic case, the lack of exact spherical symmetry of the large body (say a mountain nearby) manifests itself in a breaking of translation symmetry. This breaking leads to a dependence of V_{eff} on the other two spatial coordinates, but the corresponding terms are relatively suppressed by powers of the ratio between a parameter encoding spherical asymmetry and the large body size—the cow raises its head again.

It is in the quantum context, however, that EFTs come to full force, because virtual processes explore all possibilities allowed by symmetries. In this context it is perhaps easiest to think in terms of path integrals. When there are various possibilities for a process, the probability of the outcome is the square of the sum of the

amplitudes for each possibility, each amplitude being proportional to the exponential of $(i/\hbar)$ times the Hamilton action. After integrating over momenta, the total amplitude is expressed in terms of trajectories $q(t)$ in coordinate space as

$$A = \int \mathscr{D}q \exp\left(\frac{i}{\hbar}\int dt\,\mathscr{L}\big(q(t)\big)\right), \tag{4.9}$$

where $\mathscr{L}$ is the Lagrangian (not necessarily the classical one...). The measure $\mathscr{D}q$ stands for the sum over all possible trajectories. To make it well defined, we divide the time interval for the process in a set of discrete values t_i, $i = 0, \ldots, N$, with $t_{i+1} - t_i \equiv \hbar/(\Lambda c)$. (More complicated slicings are certainly also possible.) The action becomes a sum over each time slice and the measure is the well-defined product of integrals,

$$\int \mathscr{D}q = \prod_{i=1}^{N-1} \int dq(t_i). \tag{4.10}$$

This procedure is called regularization and the (momentum) scale Λ is referred to as the ultraviolet (UV) regulator parameter or cutoff. The classical path arises as the one that extremizes the action.

But what do we do with Λ? It is something I introduced by hand: psychology if you will, not physics. Physics is obtained from the S matrix, which is related to the scattering amplitude or the T matrix. Taking elastic two-particle scattering for simplicity, in the prototypical experiment two asymptotically free particles approach with a relative (on-shell) momentum $\mathbf{p}$ and scatter into an asymptotically free state of relative (on-shell) momentum $\mathbf{p}'$, with $|\mathbf{p}'| = |\mathbf{p}| \equiv k$ from energy conservation. The probability for the final state depends on k and the angle θ of $\mathbf{p}'$ with respect to $\mathbf{p}$. It is usually convenient to expand the θ dependence in Legendre polynomials corresponding to angular momenta $l = 0, 1, \ldots$. The coefficients $T_l(k)$ are the partial-wave amplitudes, which are usually parametrized in terms of phase shifts $\delta_l(k)$, from which the cross section can be obtained. The poles of $T_l(k)$ in the complex momentum plane can be of two types: (i) a pole in the imaginary axis, $k = i\kappa_B$, corresponding to a real ($\kappa_B > 0$) or virtual ($\kappa_B < 0$) bound state of energy $E = -B = -\kappa_B^2/2\mu + \cdots < 0$; (ii) a pair of poles elsewhere in the lower half-plane, $k = \pm\kappa_R - i\kappa_I$, $\kappa_{R,I} > 0$, representing a resonance of complex energy.

The procedure of ensuring observable quantities are independent of the regularization is called renormalization. Depending on the interactions, the most relevant paths will have structure at a certain time scale, let me call it $\hbar/Mc^2$. Certainly we want $\Lambda \gg Mc$ in order to capture the structure at this scale. But let me suppose we are interested in dynamics over a larger time scale $\hbar/mc^2$ in terms of a mass scale $m \ll M$. In this case we might be satisfied with a smaller cutoff, as long as $\Lambda \gg mc$. In the coarse-graining procedure of reducing the cutoff—called renormalization-group (RG) running—we induce errors by approximating trajectories with fine structure by a coarse set of points. We can mitigate these errors by keeping in the Lagrangian not only the positions at each slice $q(t_i)$, but also the first derivative $(dq/dt)(t_i)$ and higher derivatives, for progressively better accuracy. In

general, as discussed earlier, we also might want to change our coordinates to a new, more efficient set which is some function of the older one, $\tilde{q}(t_i) = f(q(t_i))$. This is accomplished by introducing

$$1 = \prod_i \int d\tilde{q}(t_i)\delta\big(\tilde{q}(t_i) - f\big(q(t_i)\big)\big) \equiv \int \mathscr{D}\tilde{q}\,\delta\big[\tilde{q}(t) - f_\Lambda\big(q(t)\big)\big] \tag{4.11}$$

in Eq. (4.9). Inverting the order of integrals we arrive at

$$A = \int \mathscr{D}\tilde{q}\,\exp\left(\frac{i}{\hbar}\int dt\,\mathscr{L}_{\text{eff}}\big(\tilde{q}(t)\big)\right), \tag{4.12}$$

where, schematically, the effective Lagrangian is

$$\mathscr{L}_{\text{eff}}(\tilde{q}) = \sum_{n,d,m} c_{ndm}(M,\Lambda)\,O\big(\tilde{q}^n, \big(d^d\tilde{q}/dt^d\big)^m\big). \tag{4.13}$$

Here O represents a combination of various powers of the new coordinate and its derivatives at the same instant, since we cannot resolve time intervals $\lesssim \hbar/(\Lambda c)$ because of the uncertainty principle. The respective coefficient, c_{ndm}, is called a low-energy constant (LEC), and depends in general not only on the underlying dynamics at scale M but also on the regulator Λ.

In principle the effective Lagrangian can be obtained from the integral over the original coordinates, but regardless of our ability to do so, the path integral (4.12) forms the basis for the effective theory. From it we can obtain the T matrices for various low-energy processes, the goal of effective theory being to write each in a controlled expansion. Again taking a simple two-body elastic scattering for illustration, we want that, for $k \sim mc$,

$$T_l(k) = \sum_{\nu\geq\nu_{min}}^{\infty} \tilde{c}_\nu(M,\Lambda)\left(\frac{k}{Mc}\right)^\nu F_{l;\nu}\left(\frac{k}{mc};\frac{k}{\Lambda}\right), \tag{4.14}$$

where ν is a counting index with a minimum value ν_{min}, the new coefficients $\tilde{c}_\nu$ are related to the c_{ndm} appearing in the Lagrangian, and the $F_{l;\nu}$ are calculable functions of the light scales and the cutoff, which are obtained by solving the dynamical equations (like the Schrödinger or Lippmann-Schwinger equations) of the theory. We refer to the terms with $\nu = \nu_{min}$ as leading order (LO), $\nu = \nu_{min} + 1$ as next-to-leading order (NLO), and so on. Since Λ is arbitrary, the coefficients $\tilde{c}_\nu$ (and thus the c_{ndm}) have to be such as to ensure "RG invariance",

$$\frac{dT_l(k)}{d\Lambda} = 0. \tag{4.15}$$

The relation between ν and the labels (n,d,m) of the expansion (4.13) is called power counting. Frequently the least trivial aspect of an effective theory, power counting is necessary for any predictive power. A truncation of Eq. (4.14) guarantees that only a finite number of LECs appear, but in principle introduces regularization

errors. These errors will be relatively small as long as they scale as inverse powers of k/Λ,

$$T_l(k) = T_l^{(\bar{\nu})}(k)\left[1 + \mathcal{O}\left(\frac{k}{Mc}, \frac{k}{\Lambda}\right)\right], \qquad \frac{\Lambda}{T_l^{(\bar{\nu})}(k)}\frac{dT_l^{(\bar{\nu})}(k)}{d\Lambda} = \mathcal{O}\left(\frac{k}{\Lambda}\right), \quad (4.16)$$

with $\bar{\nu}$ denoting the chosen truncation. For this to happen, there need to be enough LECs at each order to remove non-negative powers of Λ, otherwise the power counting is not consistent (with the RG). Once we have ensured that errors scale appropriately, we want at least $\Lambda \gg mc$ and, optimally, $\Lambda \gtrsim Mc$, as in the latter case the regularization errors are no larger than the errors coming from the incomplete accounting of short-range physics. In fact, as long as regulator errors come in the form (4.16) one can use a variation of Λ from Mc to very large values as an estimate of the full truncation error.

So far I have presented the ideas of EFT without invoking the notion of "field" directly, although historically they were first formalized in terms of relativistic quantum fields. The path $q(t)$ can be thought as a field over time, but closer contact with field theory arises if we "second quantize" the system, by elevating the wavefunction ψ to an operator. In the path integral formulation above one replaces

$$q(t) \to \psi(\mathbf{r}, t), \psi^*(\mathbf{r}, t), \qquad t \to \mathbf{r}, t, \qquad dt \to d\mathbf{r}dt, \quad (4.17)$$

so ψ is now a non-relativistic field over the four spacetime coordinates $\mathbf{r}, t$. Relativity can be introduced by enforcing $SO(3, 1)$ invariance, which is most easily accomplished by employing a field with definite transformation properties under the Lorentz group. We will return to the connection between relativistic and non-relativistic field theories in the next subsection. From now on I use units where $\hbar = 1$ and $c = 1$, so the dimensions of mass, energy, momentum, inverse position, and inverse time are all the same.

The EFT Lagrangian has a form similar to Eq. (4.13), which includes terms with an arbitrary number N of fields and their derivatives. It is usually convenient to discuss quantum field theory starting from an expansion around the free theory and, in non-perturbative situations, "resum" parts of this expansion. The free terms define the "canonical (mass) dimension" of the fields. With our choice of units, the action is dimensionless so each term in the Lagrangian has mass dimension 4. If an operator O has canonical dimension D, the LEC has mass dimension $4 - D$. The EFT involves interactions with arbitrary D. The terms in the expansion of the exponential of the action have a correspondence to more intuitive Feynman diagrams, which can be thought as representing the propagation of particles interspaced with their interactions. The former is represented by lines ("propagators") carrying a four-momentum and the latter by line intersections ("vertices") where four-momentum is conserved, each associated with a specific factor. A closed loop implies a free four-momentum that is integrated over. The corresponding integrals are well-defined in general only after regularization, which removes the contributions from high momenta at the cost of the arbitrary UV regulator parameter Λ. Details can be supplied by a good book on quantum field theory, such as Ref. [24].

In these terms, the recipe for an EFT is essentially:

1. identify the relevant degrees of freedom (represented by fields) and symmetries (groups of discrete or continuous, global or local transformations);
2. construct the most general Lagrangian with these ingredients;
3. postulate a power counting to truncate physical amplitudes;
4. run the methods of field theory to calculate amplitudes, that is, compute Feynman diagrams for momenta $Q < \Lambda$ (regularization) and relate the LECs to observables so that the latter are independent of Λ (renormalization);
5. if this is achieved and the now well-defined expansions are well behaved, declare victory; otherwise, return to step 3, or earlier if necessary.

Renormalization in step 4 is crucial. Short-range physics appears in both the high-momentum components of loops and in the LECs, and changes in Λ merely shuffle it from one to the other. RG invariance effectively guarantees that the relevant momenta in diagrams are set by the external momenta, so that, as long as the external momenta are relatively small, successive terms in the expansions of the various amplitudes will be smaller and smaller.

The observables used as input in step 4 can be experimental data or the result of a calculation in the underlying theory, if the latter is known and can be solved in the low-energy domain of the EFT. In this case we speak of matching the EFT to the underlying theory. When the EFT shares the symmetries of the underlying theory this matching must be possible, if one accepts Weinberg's "theorem" [18]:

> The quantum field theory generated by the most general Lagrangian with some assumed symmetries produces the most general S matrix incorporating quantum mechanics, Lorentz invariance, unitarity, cluster decomposition and those symmetries, with no further physical content.

This "theorem" has not been proved in general but to my knowledge no counterexamples are known. In specific examples, such as the one in the next subsection, one can verify that this "theorem" works.

Weinberg's "theorem" embodies the most important difference between an EFT and simple models. Models can be very useful in guiding step 1 (and sometimes 3), but they fail to be fully consistent with all the low-energy consequences of the underlying theory, which is only guaranteed with step 2. Sometimes models do contain interactions with arbitrarily many derivatives in the form of *ah hoc* "form factors" attached to vertices with otherwise no (or few) derivatives. These form factors, involving a finite number of parameters (usually one), play the dual role of representing a physical effect (the coordinate profile of a particle) and of regulating integrals. In EFT the physics of particle structure is represented by the higher-derivative interactions, each with its own LEC, while the infinities in integrals are avoided with an unphysical regulator. (Without step 4, the regulator would become indistinguishable from an universal form factor and observables would depend on Λ in addition to the infinite number of LECs that parametrize the most general Lagrangian.) A model of the underlying theory, if it includes the right symmetries, can also be represented at low energies by the EFT, with specific relations between the LECs given by the limited number of parameters of the model (including form-factor parameters, if any).

But, as long as RG invariance has been achieved, the arbitrarily higher-derivative interactions ensure that the EFT represents *all* models with the right symmetries. When the underlying theory is not known, or cannot be solved, EFT provides a model-independent approach to data.

Even when the matching of the EFT to the underlying theory can be done, there are advantages in using the EFT at low energies, because it is inefficient to keep explicit in the theory very massive degrees of freedom instead of emergent, low-mass states. No progress in nuclear theory will make it preferable to calculate atomic and molecular properties directly from a collection of protons and neutrons, rather than from a point nucleus with a few relevant parameters (which in turn can be calculated from a collection of protons and neutrons). The heavy degrees of freedom are "integrated out", their contribution subsumed in the LECs.

If the EFT is natural, one expects no cancellations between the bare LECs and the high-momentum components of loops, at least for changes in Λ of $\mathcal{O}(1)$. Now, loops typically come with factors of 4π. For a LEC c of an operator of canonical dimension D involving N fields, it is convenient to define a "reduced LEC" that is dimensionless and includes some factors of 4π,

$$c_R \equiv M^{D-4} c/(4\pi)^{N-2}. \tag{4.18}$$

It can be inferred [25, 26] from examples based on perturbative matching that c_R is usually of the order of the product of reduced couplings of the underlying theory that generate it. Examples of this "naive dimensional analysis" (NDA) will be given later, starting in the next subsection. There is no guarantee that it will always work, but it is usually at least a good first guess on which to base a power counting.

For an effective field theorist, nature has the onion-like structure of a sequence of EFTs ordered according to energy (or inverse distance) scale. (Whether this sequence ends at some high energy is metaphysics.) Thus, EFT provides a framework for both reductionism and emergence in physical theories. This and other philosophical implications of EFT are lucidly discussed in Refs. [27, 28].

In the remaining lectures I will focus on the EFT at a few GeV and its strong-interaction sector as a starting point for traditional nuclear physics. It will prove useful, however, to spend some time in the next subsection with a simpler EFT, which provides an archetype for the approach we will follow in nuclear physics.

4.2.2 An Example: NRQED

Let me now return to atoms. At a momentum scale comparable to the electron mass, the relevant degrees of freedom are electrons and nuclei interacting through the exchange of photons, as given by quantum electrodynamics (QED). As we have seen above, atomic bound states exist at a much smaller momentum scale $p_{at} \sim \alpha m_e$. Now I discuss in qualitative terms an EFT tailored to this scale [29], termed Non-Relativistic QED (NRQED) because even electrons move slowly. I will stress the features that find similar expression in the Chiral EFT of nuclei in the next lecture.

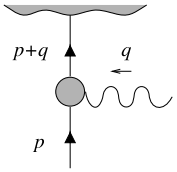

Fig. 4.1 Part of a Feynman diagram where an on-shell fermion of momentum p first interacts with a real or virtual photon of incoming momentum q, then propagates with momentum $p+q$. A fermion (photon) is denoted by a *solid* (*wavy*) *line*. The *shaded areas* represent parts of the diagram whose details are not important now

For simplicity, let me take at the higher scale a single spin-1/2 fermion represented by a Dirac field ψ of mass m and charge $Q_\psi e$, interacting with a spin-1 boson A_μ, subjected to Lorentz, parity, time-reversal, and $U(1)$ gauge invariance. As it is well known, the latter is most easily enforced using gauge-covariant derivatives:

$$D_\mu \psi = (\partial_\mu + ieQ_\psi A_\mu)\psi, \qquad F_{\mu\nu} = \partial_\mu A_\nu - \partial_\nu A_\mu. \tag{4.19}$$

The underlying Lagrangian is thus

$$\mathscr{L} = -\frac{1}{4} F_{\mu\nu} F^{\mu\nu} + \bar{\psi}(i\not{D} - m)\psi + \cdots, \tag{4.20}$$

where $\bar{\psi} = \psi^\dagger \gamma_0$ and $\not{D} = \gamma_\mu D^\mu$ in terms of the Dirac matrices γ_μ. From the terms shown explicitly in this Lagrangian we can read off the fermion and gauge-boson propagators and an interaction vertex, as discussed in textbooks [24]. More-derivative interactions, represented by the "...", give contributions suppressed by powers of momentum over the mass scale of the physics we have integrated out (such as heavier fermions and weak-gauge bosons).

If we are only interested in processes with external momenta $Q \ll m$, we can consider an additional expansion in Q/m. Take the fermion propagator after the fermion with momentum p is kicked by a photon of momentum q, see Fig. 4.1. If $|\mathbf{p}| \sim |\mathbf{q}| = \mathscr{O}(Q)$, then $q^0 \sim |\mathbf{q}| = \mathscr{O}(Q)$ but $p^0 = \sqrt{|\mathbf{p}|^2 + m^2} = m + \mathscr{O}(Q^2/m)$. The propagator can then be written

$$\frac{i}{\not{p} + \not{q} - m + i\varepsilon} = \frac{i(p^0\gamma^0 + m - \mathbf{p}\cdot\boldsymbol{\gamma} + \not{q})}{2p^0 q^0 + q^{02} - 2\mathbf{p}\cdot\mathbf{q} - \mathbf{q}^2 + i\varepsilon} = \frac{i}{q^0 + i\varepsilon} P_+ + \cdots, \tag{4.21}$$

where in the last line I introduced one of the projectors onto positive/negative energy states,

$$P_\pm \equiv \frac{1 \pm \gamma^0}{2}, \qquad P_\pm P_\pm = P_\pm, \qquad P_\pm P_\mp = 0. \tag{4.22}$$

This represents, in a first approximation, a static *two*-component fermion propagating forward in time, as can be seen from a Fourier transformation. To capture the

importance of this limited set of degrees of freedom it is convenient to split the field into two two-component "heavy fermion" fields [30]

$$\Psi_\pm \equiv e^{imt} P_\pm \psi, \qquad \psi = e^{-imt}(\Psi_+ + \Psi_-). \tag{4.23}$$

The effective Lagrangian then employs the relevant degrees of freedom embodied in Ψ_+ instead of the full ψ. It can be obtained [31] by substituting Eq. (4.23) into Eq. (4.20), integrating over the Ψ_- field in the path integral as well as the high-momentum components of Ψ_+ and A_μ, and expanding in powers of $1/m$. With an appropriate redefinition of A_μ to keep its bilinear form unchanged, and rewriting Ψ_+ as a Pauli spinor Ψ (with $\overline{\Psi} \equiv \Psi^\dagger$), the result is

$$\begin{aligned}\mathscr{L}_{NRQED} = &-\frac{1}{4}F_{\mu\nu}F^{\mu\nu} + \frac{\beta_0}{m^4}\left(F_{\mu\nu}F^{\mu\nu}\right)^2 + \frac{\beta_1}{m^4}\left(F_{\mu\nu}\tilde{F}^{\mu\nu}\right)^2 + \cdots \\ &+ \overline{\Psi} i D_0 \Psi + \frac{1}{2m}\overline{\Psi}\mathbf{D}^2\Psi + \frac{e}{2m}(Q_\psi + \kappa)\overline{\Psi}\sigma_i \Psi \tilde{F}^{0i} + \cdots \\ &+ \mathscr{L}_{f\geq 2}\end{aligned} \tag{4.24}$$

where $\tilde{F}_{\mu\nu} = \varepsilon_{\mu\nu\alpha\beta}F^{\alpha\beta}/2$, σ_i are the Pauli spin matrices, $\beta_{0,1}$ and κ are dimensionless LECs that can be obtained from the parameters appearing in Eq. (4.20), and $\mathscr{L}_{f\geq 2}$ involves four or more fermion fields, as discussed below. As one would expect, this is simply the most general Lagrangian built out of Ψ_+ and A_μ and subjected to the assumed symmetries. Invoking Weinberg's "theorem" and our experience that for $Q \ll m$ the appropriate fermion degree of freedom is a bi-spinor, one can write this Lagrangian directly, without explicitly performing a path integration. In this case, the LECs are obtained by the matching of physical amplitudes.

Even though the Lagrangian is more complicated, the structure of the EFT is much simpler than that of the underlying theory. The absence of Ψ_- implies that there is no explicit pair creation in the EFT, which is an effect of range $\sim 1/(2m)$ that is absorbed in the LECs. Fermion lines just go through Feynman diagrams of the EFT. As a consequence, operators with $2f$ fermion fields do not contribute to processes that involve less than f incoming fermions. We can tackle the various sectors of the theory successively by increasing f, which is particularly important for the treatment of non-perturbative physics for $f \geq 2$. In the relativistic theory the few-body problem is instead a many-body problem.

The $f = 0$ sector of Eq. (4.24) is the Euler-Heisenberg Lagrangian, one of the earliest examples of EFT ideas, which is the basis for studies of low-energy processes involving photon fields alone, such as light-by-light scattering. A remarkable feature of Eq. (4.24) is that it contains photon self-interactions already at tree level. The most important such interactions have four derivatives and thus by NDA are expected to be inversely proportional to m^{-4}. The LECs $\beta_{0,1}$ originate in fermion-loop diagrams of the underlying theory and would be $\mathscr{O}(1)$ if α were $\mathscr{O}(1)$. Since $\alpha \ll 1$, we can match the EFT to the underlying theory in perturbation theory, obtaining $\beta_{0,1}$ in an expansion in powers of α. The most important diagram has a single fermion loop with four photon lines attached. Since each vertex is $\propto e$ and

the loop typically brings in a $(4\pi)^{-2}$, we expect $\beta_{0,1} = \mathcal{O}(\alpha^2)$. Alternatively we can use Eq. (4.18). The reduced charge is $e_R = e/(4\pi)$ and for $c = \beta_{0,1}/m^4$ we expect $c_R = m^4 c/(4\pi)^2 = \mathcal{O}(e_R^4)$, from which, again, $\beta_{0,1} = \mathcal{O}(\alpha^2)$. One can similarly write and calculate the LECs of higher-derivative terms. They may contain further powers of α, but are additionally suppressed by at least $(Q/m)^2$ in processes with typical external momentum Q. These LECs are of course needed to ensure renormalizability, Eq. (4.16), in light-by-light scattering at loop level. An explicit comparison between EFT and QED amplitudes can be found, for example, in Ref. [32].

In the $f = 1$ sector, we see that the exponential in Eq. (4.23) removes from the evolution of the fermion field the relatively large and inert mass m, leaving a dispersion relation of the non-relativistic, "residual" form $p^0 = \mathbf{p}^2/(2m) + \cdots$. The kinetic part has a static piece $\overline{\Psi} i D_0 \Psi$, a recoil correction, and, with more derivatives, relativistic corrections. The strengths of these terms are not arbitrary, but fixed by the mass. If we neglected the "..." in Eq. (4.20) and loop corrections, the same would be true for the $\overline{\Psi}\sigma_i \Psi \tilde{F}^{0i}$ interaction, or "Pauli term", which represents the interaction of the magnetic dipole moment with a magnetic field. The existence of further physics and of radiative corrections in the underlying theory leads to an "anomalous" magnetic moment κ, which again would be expected to be of $\mathcal{O}(1)$ if α were $\mathcal{O}(1)$. The contributions from loops to κ can be estimated again using Eq. (4.18): for $c = e\kappa/m$, $c_R = mc/(4\pi) = \mathcal{O}(e_R^3) = \mathcal{O}(e^3/(4\pi)^3)$, which gives $\kappa = \mathcal{O}(\alpha/(4\pi))$, in agreement with the classic Schwinger result $\kappa = \alpha/(2\pi) + \cdots$ for the electron.

The fact that some coefficients are entirely determined by m applies also to terms contained in the "..." of Eq. (4.24), and is merely a consequence of Lorentz invariance. Despite its non-relativistic appearance, Eq. (4.24) does respect Lorentz invariance, but in a Q/m expansion. If we start directly with Eq. (4.24), rather than integrating degrees of freedom out of a manifestly Lorentz-invariant Lagrangian, Lorentz invariance can be implemented by demanding "reparametrization invariance" [33], namely that the Lagrangian should be invariant under small changes in the velocity of the heavy fermion. This method has the advantage of applying also when the relativistic version of the theory does not have a well-defined expansion and/or when the explicit integration cannot be performed explicitly. A recent discussion of the NRQED Lagrangian can be found in Ref. [34].

With the $f = 0, 1$ sectors of the Lagrangian we can study low-energy processes in which a number of photons scatter from a slow-moving fermion. As we have seen, for probe energies comparable to the fermion three-momentum, the fermion is, in a first approximation, static. We are close to the limit $m \to \infty$, where the spin operator does not appear in the Lagrangian (4.24) and there is an $SU(2)$ symmetry of rotations in spin space. This is an example of an "accidental" symmetry, a symmetry that emerges at LO in the EFT.

The simplest process is Compton scattering. In the Coulomb gauge $A_0 = 0$, the most important contribution comes from the "seagull" diagram stemming from the two $\mathbf{A}$ fields contained in $\overline{\Psi}\mathbf{D}^2\Psi$; the corresponding contribution to the amplitude, $\propto 1/m$, is nothing but the spin-independent "Thomson amplitude". In the underlying theory, this term arises from the transition to negative-energy states. One can go on

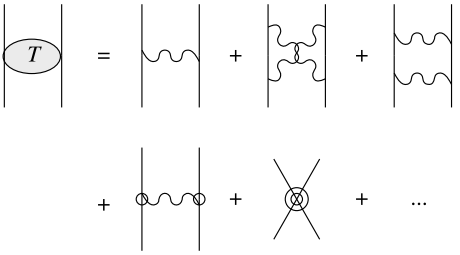

Fig. 4.2 Diagrams representing the T matrix for elastic scattering of two heavy fermions in NRQED. A *circle* at the vertex denotes an inverse power of the heavy mass. Other notation as in Fig. 4.1

and calculate higher-order terms in the combined Q/m and α expansions using the interactions in Eq. (4.24). For details at a pedagogical level, see Ref. [35].

Let me now turn to the $f \geq 2$ sectors, more germane to my goal of tackling nuclear bound states later. It is here that EFT becomes particularly useful, because the formulation of the non-perturbative problem is exceedingly complicated in the underlying theory, where we retain contributions of momentum comparable to the fermion mass. But, as we have seen, such momenta are also not very relevant for electromagnetic bound states! Here I will emphasize qualitative aspects of the problem, omitting for example a discussion of infrared divergences. For a fuller account in the case of positronium, for example, see Ref. [36].

So I consider the T matrix for the elastic scattering of two of our heavy fermions in the center-of-mass frame, where both initial and final relative three-momenta are, respectively, $|\mathbf{p}| \sim |\mathbf{p}'| = \mathcal{O}(Q)$. I will denote the transferred momentum by $\mathbf{q} \equiv \mathbf{p} - \mathbf{p}'$. See Fig. 4.2.

The simplest diagram one can draw represents the exchange of a single photon, where the photon-fermion interaction comes from the $\overline{\Psi} i D_0 \Psi$ term in Eq. (4.24). It gives

$$T_{1\gamma} = \frac{Q_\psi^2 e^2}{(p^0 - p'^0)^2 - (\mathbf{p} - \mathbf{p}')^2 + i\varepsilon} \simeq -\frac{Q_\psi^2 e^2}{\mathbf{q}^2 - i\varepsilon}\left(1 + \mathcal{O}\left(Q^2/m^2\right)\right). \tag{4.25}$$

The dominant term above, which has magnitude $\mathcal{O}(4\pi\alpha Q_\psi^2/Q^2)$, is, as we are going to see shortly, just a fancy way to generate the Coulomb potential. Of course there are other one-photon-exchange diagrams with derivatives at the vertices, which start at relative order $\mathcal{O}(Q^2/m^2)$ just like the non-static corrections in Eq. (4.25). An example comes from magnetic interactions at both vertices, which gives a dipole-dipole interaction of contact form because momenta from the vertices and propagator cancel out.

In quantum field theory, nothing forbids the exchange of more than one photon. For example, each fermion can emit a photon which is subsequently absorbed by the other fermion, forming a one-loop "crossed-box" diagram. According to the Feynman rules, the corresponding contribution is

$$T_{2\gamma\times} = -i\, Q_\psi^4 e^4 \int \frac{d^4 l}{(2\pi)^4} \frac{1}{l^0 + p^0 - (\mathbf{l} + \mathbf{p})^2/2m + i\varepsilon} \frac{1}{l^0 + p'^0 - (\mathbf{l} - \mathbf{p}')^2/2m + i\varepsilon}$$

$$\times \frac{1}{(p^0 - p'^0 + l^0)^2 - (\mathbf{p} - \mathbf{p}' + \mathbf{l})^2 + i\varepsilon} \frac{1}{l^{02} - \mathbf{l}^2 + i\varepsilon}$$

$$= Q_\psi^4 e^4 \int \frac{d^3 l}{(2\pi)^3} \frac{1}{|\mathbf{l}| - p^0 + (\mathbf{l} + \mathbf{p})^2/2m - i\varepsilon} \frac{1}{|\mathbf{l}| - p'^0 + (\mathbf{l} - \mathbf{p}')^2/2m - i\varepsilon}$$

$$\times \frac{1}{(p^0 - p'^0 - |\mathbf{l}|)^2 - (\mathbf{p} - \mathbf{p}' + \mathbf{l})^2 + i\varepsilon} \frac{1}{2|\mathbf{l}| - i\varepsilon} + \cdots . \tag{4.26}$$

Here I integrated over the zeroth component of the loop momentum using contour integration. Closing the contour on the upper plane, we get two contributions from the poles in the photon propagators, only one of which I show explicitly—the other, of a similar form, is in the "…". Because the three-momentum scale is Q, these poles lie typically a distance Q from the origin in the l^0 complex plane. As a consequence, the most important terms in the denominators after the first integration involve $|\mathbf{l}|$ and $|\mathbf{q} + \mathbf{l}|$, which, in particular, implies static fermion propagators as for $f = 1$. The propagators and integration measure typically contribute, respectively, $\mathcal{O}(Q^{-5})$ and $\mathcal{O}(Q^3/(4\pi)^2)$ to the final result, which is then $\mathcal{O}((Q_\psi^2 \alpha/4\pi)(4\pi\alpha Q_\psi^2/Q^2))$. Just as it could have been expected from experience with $f = 0, 1$ diagrams, the result is smaller than one-photon exchange by $\mathcal{O}(Q_\psi^2 \alpha/4\pi)$.

One might further expect that the smallness of α implies that all other diagrams are small and amenable to perturbation theory. However, if that were true there would be no electromagnetic bound states. So, how can a bound state arise in a weakly coupled theory? More generally, what makes the problem non-perturbative? (Since I am considering explicitly only one type of fermion, there is obviously no electromagnetic bound state because the Coulomb interaction is repulsive, but still perturbation theory fails at low energies.)

The reason is apparent already when we consider the other two-photon exchange diagram, the "box", in which the photons are exchanged sequentially. In this case there are subtle differences compared to the crossed-box diagram due to a different routing of the loop momenta in one of the fermion propagators:

$$T_{2\gamma\Box}$$

$$= -i\, Q_\psi^4 e^4 \int \frac{d^4 l}{(2\pi)^4} \frac{1}{l^0 + p^0 - (\mathbf{l} + \mathbf{p})^2/2m + i\varepsilon} \frac{1}{-l^0 + p^0 - (\mathbf{l} + \mathbf{p})^2/2m + i\varepsilon}$$

$$\times \frac{1}{(p^0 - p'^0 + l^0)^2 - (\mathbf{p} - \mathbf{p}' + \mathbf{l})^2 + i\varepsilon} \frac{1}{l^{02} - \mathbf{l}^2 + i\varepsilon}$$

$$= Q_\psi^4 e^4 \int \frac{d^3 l}{(2\pi)^3} \frac{1}{-2p^0 + (\mathbf{l} + \mathbf{p})^2/m - i\varepsilon} \frac{1}{p^0 - (\mathbf{l} + \mathbf{p})^2/2m - \mathbf{l}^2 + i\varepsilon}$$

$$\times \frac{1}{(2p^0 - p'^0 - (\mathbf{l} + \mathbf{p})^2/2m)^2 - (\mathbf{p} - \mathbf{p}' + \mathbf{l})^2 + i\varepsilon} + \cdots . \tag{4.27}$$

Because of the different signs, closing the contour on the upper half-plane now involves a third pole, which stems from one of the fermion propagators and lies only a distance Q^2/m from the origin. The contribution from this pole is the one displayed explicitly above, the other two being relegated to the "…". You should convince yourself that these other two contributions are similar to Eq. (4.26), and thus also small by $\mathcal{O}(Q_\psi^2\alpha/4\pi)$ compared to one-photon exchange. The contribution from the fermion-propagator pole, on the other hand, is larger because the remaining fermion propagator contains only the difference between small fermion kinetic energies, and is thus $\mathcal{O}(Q^2/m)$. We refer to this as an infrared enhancement, as it becomes more pronounced as Q decreases. Note that the static approximation is no longer good, although of course relativistic corrections remain small. In the photon propagators, on the other hand, the kinetic energies can still be neglected in a first approximation, so that as before each photon denominator is $\mathcal{O}(Q)$. What we have here are simply two sequential Coulomb photon exchanges separated by the usual non-relativistic two-fermion propagation: it is the iteration of one-photon exchange. Such a non-relativistic integral over the three-momentum typically contributes $\mathcal{O}(Q^3/(4\pi))$, an extra 4π compared to integrals not originating in the heavy fermion propagator poles. The size of this term is then $\mathcal{O}(Q_\psi^2\alpha m/Q)$ compared to one-photon exchange.

This argument can be generalized to diagrams with more photon exchanges, and even more fermions. It is convenient to introduce "old-fashioned" time-ordered perturbation-theory diagrams, which represent contributions to amplitudes *after* integration over the zeroth-component of loop momenta, as in the last lines in Eqs. (4.26) and (4.27). In this case vertices are drawn in a specific time order, intermediate states are associated with energy differences, and loops represent three-momentum integrations. The one-photon-exchange Feynman diagram becomes two time-ordered diagrams depending on which fermion first emits the photon. The crossed-box Feynman diagram becomes four time-ordered diagrams, all of the same crossed-box type. The box Feynman diagram becomes six time-ordered diagrams: two "stretched-box" diagrams where at any time there is a photon "in the air", representing the "…" in Eq. (4.27), and four "true-box" diagrams where there is an intermediate state without photons, representing once-iterated one-photon exchange. In this language, we define "reducible" diagrams as those that contain intermediate states with fermions only, and are thus infrared enhanced. These intermediate states contribute $\mathcal{O}(mQ/(4\pi))$ to the amplitude. The potential is defined as (minus) the sum of irreducible diagrams.

We expect the potential to have a simple perturbative expansion, which in the case considered here starts with the one-photon exchange of $\mathcal{O}(4\pi\alpha Q_\psi^2/Q^2)$. Fourier transforming Eq. (4.25), we obtain, indeed, the Coulomb potential in coordinate space. Each extra iteration of this potential adds a factor $\mathcal{O}(Q_\psi^2\alpha m/Q)$, as seen above. When $Q \sim Q_\psi^2\alpha m$, all iterations are equally important, and the amplitude is given by an integral equation, the Lippmann-Schwinger equation—which, in turn, can be shown to be equivalent to the Schrödinger equation. Schematically the LO

amplitude is

$$T^{(0)} \sim \frac{4\pi\alpha Q_\psi^2}{Q^2}\left[1-\mathcal{O}\left(\frac{Q_\psi^2\alpha m}{Q}\right)\right]^{-1}, \tag{4.28}$$

which can have a pole at $Q \sim |Q_\psi^2|\alpha m$, corresponding to energies $|E| \sim Q_\psi^4\alpha^2 m$. If we were considering two fermions with opposite charge, say $Q_\psi^2 \to -1$, we would expect a bound state with binding momentum $p_{at} \sim \alpha m$ and energy $\sim p_{at}^2/m \sim \alpha^2/m$—just the back-of-the-envelope estimate given at the beginning of this lecture.

But NRQED gives also a way to systematically go beyond LO. First, it allows us to calculate corrections to the Coulomb potential, such as the Q/m ($\sim Q_\psi^2\alpha$ in the bound state) corrections to one-photon exchange and the irreducible two-photon exchange we discussed above. Second, it tells us that these corrections to the potential are also corrections in the scattering amplitude, which should be calculated in perturbation theory on top of the LO ("distorted-wave perturbation theory").

Note that because each iteration of one-photon exchange scales with a negative power of Q, the LO amplitude (4.28) satisfies the RG condition (4.16) without invoking contact interactions in $\mathscr{L}_{f\geq 2}$. However, such four- and more-fermion terms must exist because they are allowed by the symmetries. And indeed, as the order increases and the corrections to the potential become more singular (since they have more powers of momentum or, alternatively, inverse distance), loop diagrams will bring in new cutoff dependence, which can only be compensated by the LECs. As for $f = 0, 1$, the LECs with $f \geq 2$ can in principle be obtained from a fully perturbative matching calculation in the window $m \gg Q \gg Q_\psi^2\alpha m$.

The total spin of two fermions can be $s = 0, 1$ depending on the individual spins being antiparallel or parallel. It is useful to think of the projectors onto spin s,

$$P_s \equiv \frac{1}{4}\left[2s+1+(2s-1)\sigma_1\cdot\boldsymbol{\sigma}_2\right], \qquad P_s P_{s'} = \delta_{ss'}P_s, \tag{4.29}$$

where $\boldsymbol{\sigma}_i/2$ is the spin of fermion i. Because I am considering a single two-state fermion, the Pauli principle ensures that an S-wave two-fermion contact interaction can only contribute when the spins are antiparallel. In other words, there is only one four-fermion interaction without derivatives, corresponding to P_0. The many-fermion Lagrangian has thus the form

$$\mathscr{L}_{f\geq 2} = \frac{\gamma}{4m^2}(\overline{\Psi}\Psi\overline{\Psi}\Psi - \overline{\Psi}\boldsymbol{\sigma}\Psi\cdot\overline{\Psi}\boldsymbol{\sigma}\Psi) + \cdots, \tag{4.30}$$

where γ is a LEC. NDA for $c = \gamma/m^2$ gives, assuming it accounts for photon exchange at momenta $\gtrsim m$, $c_R = m^2 c/(4\pi)^2 = \mathcal{O}(e_R^2)$ or $\gamma = \mathcal{O}(4\pi\alpha)$, suggesting a relative $\mathcal{O}(Q^2/m^2)$ effect in the two-fermion scattering amplitude. The "…" in Eq. (4.30) include not only more-derivative four-fermion interactions but also six- and more-fermion interactions, which because of their larger canonical dimensions are expected to lead to contributions suppressed by powers of Q/m. Again thanks

to the Pauli principle, for a two-state fermion there are no six- or more-fermion interactions without derivatives, which means three- and more-body forces are very small.

One can now consider arbitrary processes involving two or more fermions—in particular, in a bound state—and external low-momentum photons, for example *Bremsstrahlung*. NRQED provides the framework to describe atomic and molecular physics, and indeed state-of-the-art calculations are carried out within this framework (Ref. [37] is but one example). I will now set up an analogous framework for nuclear physics.

4.2.3 Summary

Nuclear systems involve multiple scales but no obvious small coupling constant. EFT is a *general* framework to deal with multi-scale problems using small ratios of scales as expansion parameters. Applied to low-energy QED, EFT reproduces some well-known results but also provides a systematic expansion for scattering amplitudes.

4.3 QCD at Low Energies

For the rest of these lectures I apply the EFT framework to nuclear systems. I start with the Standard Model (SM) of particle physics at a few GeV and construct the EFT relevant for momenta $\mathcal{O}(M_{nuc})$, which should form the basis for a description of typical nuclei. This Chiral EFT has indeed become the starting point for the rapidly developing "*ab initio*" methods that harness ever-growing computational power for the solution of the nuclear dynamics from interactions determined in few-nucleon systems. However, as we are going to see in some detail, some basic issues in this EFT, related to the impact of the renormalization of singular potentials on power counting, are still not fully understood.

4.3.1 Building Blocks

The SM has been repeatedly validated, particularly at scales above a few GeV where most processes can be studied with relatively little reliance on non-perturbative physics. The successes of the SM can be understood if it is considered as an EFT at energies around 100 GeV. It is constructed (in its minimal version) out of quarks, leptons, gauge bosons and a Higgs boson subjected to an $SU(3)_c \times SU(2)_L \times U(1)_Y$ gauge symmetry. All interactions of canonical dimension up to four have now been established directly or indirectly, and the only allowed dimension-five operator,

which violates lepton number, is a candidate to explain the small neutrino masses. Operators of dimension six and higher can cause smaller effects still, for example baryon-number violation.

As the energy scale is lowered, we can integrate out the Higgs and weak-gauge bosons, which leaves as only gauge symmetries the $SU(3)_c$ of color and the electromagnetic $U(1)_{em}$, for which the force carriers are, respectively, eight gluons $G_\mu \equiv G_\mu^a \lambda^a$, with λ^a, $a = 1, \ldots, 8$, the Gell-Mann $SU(3)$ matrices and sum over a implied, and the photon A_μ. Likewise, we can integrate out the heaviest quarks (top, bottom, charm). Although not irrelevant for nuclear physics, strange quark effects are not dominant for ordinary nuclei because, as we are going to see, in a hadronic theory the quark masses come together with the relatively large scale M_{QCD}. If the strange quark is kept explicit in the theory, the relatively heavy strange hadrons pose significant difficulties to the convergence of the low-energy EFT. In contrast, if the strange quark is integrated out, as I will do, its effects are suppressed by the strange hadron masses. The relevant quark fields are then conveniently written as an isospin doublet,

$$q = \begin{pmatrix} u \\ d \end{pmatrix}. \tag{4.31}$$

Here u and d are Dirac spinors for the up and down quarks, taken to be mass eigenstates with real masses $m_u = \bar{m}(1-\varepsilon)$ and $m_d = \bar{m}(1+\varepsilon)$. Matrices in isospin space can be expressed in terms of the unit matrix, which I will not write explicitly, and the isospin Pauli matrices τ_a, $a = 1, 2, 3$. Quarks transform under $U(1)_{em}$ according to the charge matrix

$$Q_q = \begin{pmatrix} 2/3 & 0 \\ 0 & -1/3 \end{pmatrix} = \frac{1}{6}(1 + 3\tau_3) \tag{4.32}$$

and under $SU(3)_c$ with a universal strength g, which also governs gluon self-interactions. If we define the covariant derivatives

$$D_\mu q = (\partial_\mu + ie Q_q A_\mu - ig G_\mu) q, \qquad G_{\mu\nu} = \partial_\mu G_\nu - \partial_\nu G_\mu + ig[G_\mu, G_\nu], \tag{4.33}$$

the most general Lagrangian with Lorentz invariance and these gauge symmetries is (see, *e.g.*, Ref. [38])

$$\begin{aligned} \mathscr{L}_{QCD} = & -\frac{1}{4} F_{\mu\nu} F^{\mu\nu} - \frac{1}{2} \mathrm{Tr}\left\{ G_{\mu\nu} G^{\mu\nu} \right\} + \bar{q} i \not{D} q \\ & - \bar{m}\, \bar{q} \left[1 - \varepsilon \tau_3 + \frac{1-\varepsilon^2}{2} \bar{\theta}\, i\gamma_5 \right] q + \cdots \end{aligned} \tag{4.34}$$

where $\bar{\theta}$ is the so-called QCD vacuum angle (assumed to be small on phenomenological grounds) and "..." represent higher-dimensional operators. For simplicity I have dumped into the "..." also leptonic terms, whose virtual importance in purely hadronic process is small. They are of course needed when considering processes with external leptons, which I will not do explicitly in these lectures.

In order to understand some of the low-energy consequences of the theory based on the Lagrangian (4.34), I will first neglect the "…", in which case I am left with five parameters: g, $\bar{m}$, ε, e, and $\bar{\theta}$. I will argue based on *a posteriori* agreement with phenomenology that the last four parameters can, in some sense, be considered small. I will start with the "chiral limit" in which they are all set to zero, and then consider the changes their non-vanishing values cause. Some of this material (and original references) can be found in a good advanced textbook, such as Ref. [39].

4.3.1.1 Chiral Limit

In the chiral limit QCD has a single *dimensionless* parameter, g, and the action is invariant under scale transformations ($x \to \lambda^{-1}x$, $q \to \lambda^{3/2}q$, $G_\mu \to \lambda G_\mu$, $A_\mu \to \lambda A_\mu$, with λ a real parameter). However, in the path integral obtained from $\mathscr{L}_{QCD}$, scale invariance is "anomalously" broken by the inevitable presence of a *dimensionful* regulator. For renormalization, the strong constant $\alpha_s \equiv g^2/4\pi$ "runs" with the energy scale: it decreases as the energy increases—"asymptotic freedom"—and conversely increases as the energy decreases, so that $\alpha_s(1\,\text{GeV}) \sim 1$. Assuming "confinement", that is, that only colorless states ("hadrons") are asymptotic, and naturalness, the fact alluded to in the previous lecture that *almost* all hadrons have masses $\mathscr{O}(1\text{ GeV})$ indicates that QCD has a characteristic scale $M_{QCD} \sim 1$ GeV.

I seek here the EFTs of QCD for momenta $Q \ll M_{QCD}$. The first clue comes from the observation that the three pions—the lightest mesons—form a nearly degenerate isospin triplet,

$$\vec{\pi} = \begin{pmatrix} (\pi^+ + \pi^-)/\sqrt{2} \\ -i(\pi^+ - \pi^-)/\sqrt{2} \\ \pi^0 \end{pmatrix}, \tag{4.35}$$

of pseudoscalar mesons with an approximate common mass $m_\pi \simeq 140$ MeV $\ll M_{QCD}$. Would this be an indication of a breakdown in the naturalness assumption? No! The smallness and near degeneracy of pion masses can be naturally explained if we assume the "spontaneous" breaking of "chiral symmetry".

If I define the projectors

$$P_{L,R} \equiv \frac{1 \mp \gamma_5}{2}, \qquad P_{L,R}P_{L,R} = P_{L,R}, \qquad P_{L,R}P_{R,L} = 0, \tag{4.36}$$

I can split the quark field into two components

$$q_{L,R} \equiv P_{L,R}q, \quad q = q_L + q_R. \tag{4.37}$$

In the limit I am considering, the quarks are massless and can have a definite left (L) or right (R) chirality according to its spin being against or in the direction of the momentum. Moreover, in this limit the quark kinetic term in $\mathscr{L}_{QCD}$ splits into two

terms, which involve q_L and q_R separately. Each term is invariant under a separate $SU(2)$ transformation in isospin space, so $\mathscr{L}_{QCD}$ has a global $SU(2)_L \times SU(2)_R$ chiral symmetry. Since $SU(2)_L \times SU(2)_R$ is the covering group of $SO(4)$, it is sometimes sufficient to consider the latter, more intuitive group.

However, chiral symmetry is certainly not realized in the low-mass hadronic spectrum, where the lightest scalar meson and the lowest negative-parity spin-1/2 baryon have masses that are several hundreds of MeV above pions and nucleons, respectively. Still, the spectrum can be qualitatively understood if I assume that the solution of the path integral has, instead, a smaller, global symmetry of isospin given by the diagonal subgroup $SU(2)_{L+R}$, when again it is sometimes easier to talk instead of $SO(3)$. Goldstone's theorem tells us that there are massless (pseudo)scalars in the coset space $SO(4)/SO(3)$. The phenomenon here is completely analogous to the spontaneous breaking of $SO(3)$ rotational invariance down to $SO(2)$ that gives rise to spontaneous magnetization and spin waves in a ferromagnet.

An intuitive picture of this effect comes from considering the effective potential of QCD in the mesonic sector, as function of the four components of the $SO(4)$ vector

$$S = \begin{pmatrix} -i\bar{q}\gamma_5 \overrightarrow{\tau} q \\ \bar{q}q \end{pmatrix}. \tag{4.38}$$

$SO(4)$ symmetry of the potential means that it is invariant under rotations of S. If the potential had a minimum at the origin, $SO(4)$ would be manifest in the spectrum. Non-perturbative physics in QCD must be such as to make the potential have instead a "Mexican hat" shape: a degenerate set of absolute minima—a four-dimensional "chiral circle"—a distance away from the origin, which defines the pion decay constant f_π. If we take the "true" minimum to be in the $\bar{q}q$ direction, there are three massless excitations in the $\bar{q}i\gamma_5\tau_a q$ directions, which we can identify as the pions. In contrast, in the $\bar{q}q$ direction there is curvature in the potential, which we could expect to be characterized by M_{QCD} so that the corresponding scalar "sigma" meson has a mass $m_\sigma \sim M_{QCD}$.

The massless pions, but not excitations with mass $\mathcal{O}(M_{QCD})$, need to be accounted for explicitly in the EFT, since they give rise to long-distance interactions. In the limit we are considering, $SO(4)$ is an exact symmetry of the dynamics, so the EFT Lagrangian has to be invariant under small $SO(4)$ rotations, which are pion-field translations $\overrightarrow{\pi} \to \overrightarrow{\pi} + \overrightarrow{\varepsilon}$, with ε_i three constants. The simplest way to implement the symmetry is to choose pion fields such that all their interactions involve $\partial_\mu \overrightarrow{\pi}$, although, the manifold being a circle, a derivative is always accompanied by a factor of $(1 - \overrightarrow{\pi}^2/4f_\pi^2 + \cdots)$. Because there are only three pions, $SO(4)$ cannot be realized linearly, but there is a well-developed technology to incorporate chiral symmetry in the Lagrangian, the theory of non-linear realizations of symmetries [39]. Pions and fermion fields transform non-linearly, but covariant derivatives can

be defined which transform in a simple way:

$$\begin{aligned} D_\mu \vec{\pi} &= \left(1 - \frac{\vec{\pi}^2}{4f_\pi^2} + \cdots\right)\partial_\mu \vec{\pi}\,, \\ \mathscr{D}_\mu \psi &= \left(\partial_\mu + \frac{i}{2f_\pi^2}\vec{I}_\psi \cdot \vec{\pi} \times D_\mu \vec{\pi}\right)\psi, \end{aligned} \tag{4.39}$$

where $\vec{I}_\psi$ is the generator of isospin in the representation of the fermion ψ (*e.g.* $\vec{I}_N = \vec{\tau}/2$ for the nucleon field N). Similarly one can define covariant derivatives of the covariant derivatives, and so on. Under the full chiral group these derivatives transform as under the unbroken isospin subgroup, but with a pion-field-, and thus position-, dependent parameter. The consequence is that an interaction built of these covariant ingredients to be isospin symmetric is automatically chiral invariant.

Each chiral-invariant effective interaction will have its LEC. Since the QCD dynamics that generate them is non-perturbative, they should contain arbitrary powers of g. As far as NDA goes, that means reduced couplings with arbitrary dependence on $g_R \equiv g/4\pi$. Thus consistency requires that we take $g_R \sim 1$, and thus a LEC of a chiral-invariant operator of canonical dimension D involving N fields is expected to be $c = \mathscr{O}((4\pi)^{N-2}/M_{QCD}^{D-4})$. Even though these LECs might not be particularly small, chiral-invariant interactions become weak at sufficiently low energies because each derivative brings in a power of momentum Q. And, for interactions with fixed N, NDA suggests that an extra derivative gives a relative factor Q/M_{QCD}. As we are going to see, this is a good guide for the perturbative sector of the EFT, but it is not always true in the nuclear sector where the EFT is non-perturbative.

4.3.1.2 Away from the Chiral Limit

Pions are, however, not massless. Let me take a second step and consider $\bar{m} \neq 0 \ll M_{QCD}$, but still $\varepsilon = 0$, $e = 0$, and $\bar{\theta} = 0$. Now there is an explicit breaking of chiral symmetry in Eq. (4.34), since $\bar{q}q$ is one of the components of the $SO(4)$ vector S in Eq. (4.38). The Lagrangian is still invariant under the $SO(3)$ isospin subgroup.

In the Mexican-hat picture, the effect of this term is to lower (raise) the potential in the direction of positive (negative) $\bar{q}q$, breaking the degeneracy of the now-deformed chiral circle. We can still talk of a tilted, approximately circular bottom of the hat, with a slightly different radius $f_\pi \simeq 92$ MeV. The distorted potential shape should not greatly affect the mass of the sigma or any other non-Goldstone state. But because the bottom is no longer flat, pions acquire a mass, and we speak of them as pseudo-Goldstone bosons. Note that it is the explicit breaking of chiral symmetry that justifies our choice of true vacuum in the chiral limit. Spontaneous breaking of a continuous symmetry only exists in a well-defined limit of the explicitly broken case. In a ferromagnet, this "vacuum alignment" is manifest in a spontaneous magnetization in the direction of a previously applied magnetic field.

In the EFT with pions, the Lagrangian no longer has $SO(4)$ invariance; there are now terms that break chiral symmetry in the $\bar{q}q$ direction, that is, the fourth

component of S. Such terms do not necessarily contain derivatives but are proportional to powers of $\bar{m}$—actually $\bar{m}_R \equiv \bar{m}/M_{QCD}$ if we invoke NDA. One example is the pion mass term, for which we expect $m_\pi^2 = \mathcal{O}(M_{QCD}\bar{m})$, since from Eq. (4.18) $(m_\pi^2)_R \equiv m_\pi^2/M_{QCD}^2 = \mathcal{O}(\bar{m}_R)$. This roughly gives an average quark mass in the ballpark of 10 MeV. Another example is the so-called nucleon sigma term, the leading change Δm_N in the nucleon mass away from the chiral limit: by NDA $(\Delta m_N)_R \equiv \Delta m_N/M_{QCD} = \mathcal{O}(\bar{m}_R)$, or $\Delta m_N = \mathcal{O}(\bar{m}) = \mathcal{O}(m_\pi^2/M_{QCD})$. Terms with higher powers in $\bar{m}$ come from the fourth components of tensor products of S. In this way we are able to produce an S matrix with the correct chiral-symmetry breaking, not restricted to first-order in the breaking parameters. For details of how to construct these operators, see Refs. [38, 39].

The low-energy effects of the remaining terms in Eq. (4.34) can be analyzed in similar fashion [38]. When we allow $\varepsilon \neq 0$, even the $SO(3)$ group of isospin is explicitly broken, since the corresponding term in Eq. (4.34) transforms as the third component of another $SO(4)$ vector,

$$P = \begin{pmatrix} \bar{q}\overrightarrow{\tau} q \\ i\bar{q}\gamma_5 q \end{pmatrix}. \tag{4.40}$$

In the EFT Lagrangian, this means there is going to be another class of terms that break isospin like $\bar{q}\tau_3 q$, which are proportional to powers of $\varepsilon\bar{m}$—in fact $(\varepsilon\bar{m})_R \equiv \varepsilon\bar{m}/M_{QCD}$ according to NDA. An example is the quark-mass contribution to the neutron-proton mass difference: from NDA, $(\delta m_N)_R \equiv \delta m_N/M_{QCD} = \mathcal{O}((\varepsilon\bar{m})_R)$ or $\delta m_N = \mathcal{O}(\varepsilon\bar{m}) = \mathcal{O}(\varepsilon m_\pi^2/M_{QCD})$. Among terms of higher order in the symmetry-breaking parameters one finds a contribution to the pion mass splitting, which by NDA is expected to be $\delta m_\pi^2 = \mathcal{O}((\delta m_N)^2)$.

Allowing for $e \neq 0$ introduces further isospin breaking since the photon couples differently to up and down quarks. There result two types of interactions in the EFT. First, "soft" photons interact in the standard NRQED fashion with other low-energy degrees of freedom: either through $U(1)$ covariant derivatives, with

$$\partial_\mu \pi_a \to (\delta_{ab}\partial_\mu + e\varepsilon_{3ab}A_\mu)\pi_b, \qquad \partial_\mu \psi \to (\partial_\mu + ieQ_\psi A_\mu)\psi \tag{4.41}$$

in Eq. (4.39), or through $F_{\mu\nu}$. In either case, the interactions are proportional to e. Second, "hard" photons, which are integrated out, give rise to purely hadronic interactions with strengths proportional to $e_R^2 = \alpha/4\pi$. In this case chiral symmetry is broken as the 34-component of the $SO(4)$ antisymmetric tensor

$$T_\mu = \begin{pmatrix} \varepsilon_{abc}\bar{q}\gamma_\mu\gamma_5\tau_c q & \bar{q}\gamma_\mu\tau_b q \\ -\bar{q}\gamma_\mu\tau_a q & 0 \end{pmatrix}. \tag{4.42}$$

Among the effects from hard photons one finds contributions to both the pion mass splitting and the neutron-proton mass difference. From NDA, since both are expected to require at least one photon exchange, for the former $\bar{\delta} m_\pi^2 = \mathcal{O}(\alpha M_{QCD}^2/(4\pi))$ and for the latter $\bar{\delta} m_N = \mathcal{O}(\bar{\delta} m_\pi^2/M_{QCD})$.

In order to isolate the quark mass difference encoded in ε, one should look at quantities that depend linearly on ε, such as the neutron-proton mass difference.

It is useful to focus on a discrete subgroup of $SO(3)$, called charge symmetry, of rotations that interchange up and down quark (up to a sign). Observables that are charge-symmetry breaking are linear in ε, because the ε term in Eq. (4.34) changes when up and down quark are interchanged. Electromagnetism also breaks charge symmetry, so its effects have to be estimated. When this is done, one finds $\varepsilon \sim 1/3$ [40]. Observables that are isospin but not charge-symmetry breaking—sometimes called "charge-independence" breaking—are proportional to ε^2 at best, so are usually dominated by electromagnetic effects. NDA suggests that this is the case, for example, for the pion mass splitting.

In the next step we allow $\bar{\theta} \neq 0$. The corresponding term in Eq. (4.34) now breaks both parity (P) and time-reversal (T) invariance. To arrive at this term I have followed Ref. [41] and performed an anomalous chiral rotation to eliminate a term of the type $\mathrm{Tr}\{G_{\mu\nu}\tilde{G}^{\mu\nu}\}$ that leads to T violation through non-perturbative effects. There is an infinite number of rotations that perform this task, but I have selected the one for which the vacuum is stable. The form in Eq. (4.34) is useful because it shows that the $\bar{\theta}$ term leads also to chiral-symmetry breaking, as the fourth component of the *same* $SO(4)$ vector P that appears in quark-mass isospin violation, Eq. (4.40). In the EFT, thus, there is a intimate relationship between the strengths of T-violating and those of T-conserving, charge-symmetry-breaking interactions [38]. Exploiting this connection and assuming naturalness in Chiral EFT, we can convert the tight limit on the neutron electric dipole moment [42] to a bound $\bar{\theta} \lesssim 10^{-10}$. Why $\bar{\theta}$ is so much smaller than 1 is an open naturalness problem in the SM, known as the strong CP problem. (Assuming CPT is a good symmetry, T violation implies CP violation and *vice-versa*.)

Finally, one can go on and construct the low-energy interactions coming from the higher-dimensional operators in the "…" in Eq. (4.34), such as P- [43, 44] (and T- [45]) violating interactions stemming from dimension-four (and -six) interactions in the SM.

All the EFT interactions that originate beyond the basic quark-gluon interaction are proportional to powers of relatively small parameters: $\bar{m}/M_{QCD}$, $\varepsilon\bar{m}/M_{QCD}$, e, $\alpha/(4\pi)$, *etc.* Thus, these interactions also tend to be weak, so that the full EFT allows for a controlled expansion of hadronic amplitudes. But obviously I am not being precise here. We have already seen, for example, how inverse powers of Q can compensate for the smallness of α at low energies to give rise to electromagnetic bound states. We are going to witness a failure of a simple perturbative expansion in nuclei as well. In both cases, however, an expansion still exists on top of a non-perturbative LO.

4.3.2 Chiral EFT

I am now in position to formulate Chiral EFT. The goal is to describe nuclear processes with typical external momenta $Q \sim M_{nuc} \ll M_{QCD}$ consistently with QCD. I start by building the chiral Lagrangian and then discuss at a qualitative level its implications, as we did for NRQED.

4.3.2.1 Chiral Lagrangian

At a minimum, we need to include the lightest baryons, the proton and neutron, which are (at least nearly) stable in the time scale of strong-interaction processes. Just as in NRQED, we can include only their two non-relativistic components, since pair creation requires $\gtrsim 2m_N \sim M_{QCD}$ in energy. At $Q \sim m_\pi$ we are probing distances at which pion-exchange effects can be resolved, so the three pions are also relevant degrees of freedom. In contrast, all other mesons can be integrated out because they have masses $\mathcal{O}(M_{QCD})$. If we are interested in going a bit further in energy, or increase the convergence of the theory at low energies, we should also include nucleon excitations. The four charge states of the isospin-3/2, spin-3/2 Delta isobar have approximately equal masses, with $m_\Delta - m_N \sim 3f_\pi$, which numerically is about $2m_\pi$. One should thus expect considerable effects from the Delta, which are best reproduced if the Delta is not integrated out but instead kept explicitly as a heavy fermion field, from which we remove the same phase as for the nucleon field. (It is not difficult to generalize the heavy fermion formalism to spin higher than 1/2.) It is convenient to include also an explicit field for the next excitation, the Roper, which has the same quantum numbers of the nucleon, even though with $m_R - m_\Delta \sim 2f_\pi$ we are getting close to M_{QCD}. For simplicity, here I omit the Roper and other nucleon resonances. My baryon fields are thus

$$N = \begin{pmatrix} p \\ n \end{pmatrix}, \qquad \Delta = \begin{pmatrix} \Delta^{++} \\ \Delta^{+} \\ \Delta^{0} \\ \Delta^{-} \end{pmatrix}. \tag{4.43}$$

In order to couple the nucleon to the Delta, one introduces [10] 2×4 spin and isospin transition operators, respectively $\mathbf{S}$ and $\overrightarrow{T}$, normalized so that $S_i S_j^\dagger = (2\delta_{ij} - i\varepsilon_{ijk}\sigma_k)/3$ and analogously for $\overrightarrow{T}$.

The next step is to write the most general Lagrangian with the same symmetry structure as QCD: Lorentz, $SU(3)_c$, $U(1)_{em}$, and approximate, spontaneously broken $SU(2)_L \times SU(2)_R$. I will consider explicitly here only the terms shown in Eq. (4.34) with $\bar{\theta} = 0$, in which case P and T are also symmetries. This is sufficient for describing the essence of nuclear physics, but of course one can later add interactions reflecting the neglected terms, which give rise to smaller (but sometimes important!) effects from weak interactions and physics beyond the SM. Color gauge invariance is trivial because every field is a singlet. Lorentz and electromagnetic gauge invariance can be implemented in the usual way, as we have done in NRQED. Chiral symmetry is a bit less familiar, but is implemented as described in the previous subsection. It is important to notice that in QCD chiral symmetry is broken in a specific way, which is reproduced in the EFT. In contrast, most hadronic models do not account for the correct pattern of chiral-symmetry breaking.

Each interaction in the chiral Lagrangian has a LEC, which in principle can be obtained from a direct calculation of QCD amplitudes at low energies, for example

using lattice simulations. In fact, since in Chiral EFT the quark masses can be varied independently, EFT amplitudes can be matched to lattice QCD amplitudes at the somewhat larger quark masses amenable to today's computers. Chiral EFT provides an extrapolation tool to smaller quark masses, and can be used to pre- or post-dict observables at the long distances not accessible directly in lattice QCD. For the time being, however, one has to resort to fitting LECs to experimental, rather than lattice, data.

In any case, we need to start with an assumption about the sizes of the LECs, so as to calculate amplitudes in the EFT before matching them to data. I assume NDA, Eq. (4.18), with $M = M_{QCD}$, and take $f_\pi = \mathcal{O}(M_{QCD}/4\pi)$ and $m_\Delta - m_N$ as low-energy scales. In addition to an expansion in powers of momenta and $m_\Delta - m_N$, there are separate expansions in the chiral-breaking parameters $\bar{m}/M_{QCD}$, $\varepsilon\bar{m}/M_{QCD}$, e, $\alpha/(4\pi)$, *etc.* How we combine them with the expansion of chiral-invariant operators is to some extent a matter of choice. The first parameter can be converted into m_π^2/M_{QCD}^2 and paired with the momentum expansion for $Q \sim m_\pi$. The second parameter, now $\varepsilon m_\pi^2/M_{QCD}^2$, depends on the dimensionless number $\varepsilon \sim 1/3$. Although one can certainly entertain a counting where ε is taken as comparable to $\mathcal{O}(m_\pi/M_{QCD})$, I prefer to err on the side of overestimating rather than underestimating isospin breaking and count it as $\mathcal{O}(1)$. Similar choices affect the electromagnetic interactions. Since e appears explicitly in covariant derivatives, it is natural to count it as Q. On the other hand, $\alpha/4\pi$ is numerically not very far from $\varepsilon m_\pi^3/M_{QCD}^3$, so having chosen $\varepsilon = \mathcal{O}(1)$ leaves $\alpha/4\pi$ as giving suppression comparable to three powers of the expansion parameter. (Anything less would make the pion mass splitting appear in LO, clearly too much of overestimate.)

With these choices, it is convenient to write the chiral Lagrangian as

$$\mathscr{L}_{ChEFT} = \sum_{\Delta=0}^{\infty} \mathscr{L}_{f=0,1}^{(\Delta)} + \mathscr{L}_{f\geq 2}, \tag{4.44}$$

where I introduced the "chiral index" [2, 18]

$$\Delta = d + f - 2 \geq 0 \tag{4.45}$$

of an interaction with d derivatives and powers of m_π or $m_\Delta - m_N$ or e or $(\alpha/4\pi)^{1/3}$, and $2f$ fermion fields. This index counts inverse powers of the high scale M_{QCD}—even for hard-photon operators, as long as we count $\alpha/4\pi \sim \varepsilon m_\pi^3/M_{QCD}^3$. It is bounded from below because chiral symmetry guarantees that terms with $f = 0$ have at least two derivatives or powers of m_π and thus $d = 2$, while terms with $f = 1$ have at least one derivative and thus $d = 1$:

$$\begin{aligned}\mathscr{L}_{f=0,1}^{(0)} = &\frac{1}{2}(D_\mu \vec{\pi})^2 - \frac{m_\pi^2}{2}\vec{\pi}^2\left(1 - \frac{\vec{\pi}^2}{4f_\pi^2} + \cdots\right) - \frac{1}{4}F_{\mu\nu}F^{\mu\nu} \\ &+ \bar{N}iD_0 N + \frac{g_A}{2f_\pi}\bar{N}\vec{\tau}\boldsymbol{\sigma}N\cdot\mathbf{D}\vec{\pi}\end{aligned}$$

$$+\bar{\Delta}\big[i\mathscr{D}_0-(m_\Delta-m_N)\big]\Delta$$
$$+\frac{h_A}{2f_\pi}[\bar{N}\overrightarrow{T}\mathbf{S}\Delta+\text{H.c.}]\cdot\cdot\mathbf{D}\overrightarrow{\pi}+\cdots \tag{4.46}$$

where g_A and h_A are LECs, and "..." contain terms with more pion and/or Delta fields. Increasing the chiral index we find

$$\begin{aligned}
\mathscr{L}^{(1)}_{f=0,1}=&-\frac{\bar{\delta}m_\pi^2}{2}\left(\overrightarrow{\pi}^{\,2}-\pi_3^2\right)\left(1-\frac{\overrightarrow{\pi}^{\,2}}{2f_\pi^2}+\cdots\right)\\
&+\bar{N}\left[\frac{\mathscr{D}^2}{2m_N}+\Delta m_N\left(1-\frac{\overrightarrow{\pi}^{\,2}}{4f_\pi^2}+\cdots\right)\right.\\
&\left.-\frac{\delta m_N}{2}\left(\tau_3-\frac{1}{2f_\pi^2}\pi_3\overrightarrow{\pi}\cdot\overrightarrow{\tau}+\cdots\right)\right]N\\
&+\frac{1}{f_\pi^2}\bar{N}\big[b_1(D_0\overrightarrow{\pi})^2-b_2(\mathbf{D}\overrightarrow{\pi})^2+ib_3\varepsilon_{ijk}\varepsilon_{abc}(D_i\pi_a)(D_j\pi_b)\sigma_k\tau_c\big]N\\
&-\frac{g_A}{4m_N f_\pi}[i\bar{N}\overrightarrow{\tau}\boldsymbol{\sigma}\cdot\mathscr{D}N+\text{H.c.}]\cdot D_0\overrightarrow{\pi}\\
&-\frac{h_A}{4m_N f_\pi}[\bar{N}\overrightarrow{T}\mathbf{S}\cdot\mathscr{D}\Delta+\text{H.c.}]\cdot D_0\overrightarrow{\pi}\\
&+\frac{e}{4m_N}\bar{N}\left\{1+\kappa_0\right.\\
&\left.+(1+\kappa_1)\left[\tau_3-\frac{1}{2f_\pi^2}\left(\overrightarrow{\pi}^{\,2}\tau_3-\pi_3\overrightarrow{\pi}\cdot\overrightarrow{\tau}\right)+\cdots\right]\right\}\sigma_i N\tilde{F}^{0i}\\
&+\cdots,
\end{aligned} \tag{4.47}$$

where $\kappa_{0,1}$ and $b_{1,2,3}$, are new LECs, and so on.

Equations (4.46) and (4.47) are sufficient to illustrate some of the characteristics of Chiral EFT. First, notice that the electromagnetic interactions are similar to those in NRQED (4.24) once we account for the isospin of the nucleon. For example, the anomalous magnetic moment of the proton (neutron) is $\kappa_{p(n)}=[\kappa_0+(-)\kappa_1]/2$. Terms like the $\beta_{0,1}$ in Eq. (4.24) appear only at higher orders. Second, the pions play a role in Chiral EFT similar to the photon in NRQED, in the sense that they are relativistic bosons that self-interact, dress and can be exchanged among fermions. Third, the fermions themselves are non-relativistic and therefore the theory can likewise be split into sectors of different fermion numbers. But, as stressed before, the theory *is* Lorentz invariant, with invariance implemented in a Q/m_N expansion, as revealed by the terms in Eq. (4.47) whose coefficients are determined by the LECs from Eq. (4.46) and m_N.

4.3.2.2 Chiral Perturbation Theory

Just like NRQED, Chiral EFT is perturbative in the sectors of $f = 0, 1$, where it is referred to as Chiral Perturbation Theory (ChPT). For a more complete introduction and references see, for example, Ref. [46].

Let us consider an arbitrary scattering process involving $A = 0, 1$ nucleon and one or more incoming and outgoing pions and photons, all with external three-momenta $Q = \mathcal{O}(M_{nuc})$. In this case, after renormalization all internal three-momenta in loops can also be taken as comparable to Q. Important for perturbation theory is the energy difference between an intermediate state and the initial state, and that is also of $\mathcal{O}(Q)$. Using topological identities about Feynman diagrams, one can show that the amplitude can be put in the schematic form of Eq. (4.14) with [2]

$$\nu = 2 - A + 2L + \sum_i V_i \Delta_i \geq 2 - A \equiv \nu_{min}, \tag{4.48}$$

where L is the number of loops, V_i is the number of vertices of type i, which have chiral index Δ_i, and the sum is over all types of vertices. The lower bound, stemming from the lower bound on the chiral index (thus ultimately from chiral symmetry) means that LO consists of all tree diagrams that can be constructed out of $\mathscr{L}^{(0)}$, NLO from tree diagrams with one insertion of a $\mathscr{L}^{(1)}$ element, *etc.* Loops start contributing at $\mathrm{N^2LO}$. The tree results are equivalent to old current algebra, but ChPT allows a systematic exploration of quantum corrections. One should of course keep in mind that this power counting is meant as a general guide; for a specific process at specific kinematics there might be a reorganization of the ordering that better reflects the relative importance of interactions.

The ChPT expansion in Q/M_{QCD} actually comprises: (i) a non-relativistic expansion for fermions in Q/m_N; (ii) a multipole expansion of the "heavy" meson cloud in $Q/m_\sigma, \ldots$; and (iii) a pion-loop expansion in even powers of $Q/(4\pi f_\pi)$. Resumming any of these three expansions would be great, but would not affect the overall error of a truncation unless the other two expansions can be resummed at the same time. As noted, since m_N is not smaller than the other high scales, it does not increase the error to include Lorentz invariance only approximately. Conversely, the error is not decreased in covariant versions of ChPT. Although we are not solving QCD at short distances, which might well be represented by a very dense cloud of heavy mesons, we are exploiting the fact that this "inner" cloud is short-ranged at the resolution scale $1/Q$. At this scale the pion cloud is not short-ranged and cannot be treated in a multipole expansion, but the large factor $4\pi f_\pi$ associated with loops means that the "outer" pion cloud is sparse, the probability of finding pions "in the air" decreasing with increasing number.

The $f = 0$ sector describes interactions of pions and photons. Already at LO pions self-interact via the kinetic and mass terms in Eq. (4.46), with strengths determined by f_π and m_π, a classic result due to Weinberg. At relative $\mathcal{O}(Q^2/M_{QCD}^2)$, there are further self-interactions with two extra derivatives, analogous to the $\beta_{0,1}$ terms in Eq. (4.24), which provide counterterms for the one-loop diagrams at the

same order. When considering isospin-violating quantities one needs to account for the pion mass splitting from Eq. (4.47) as well. Nowadays calculations have reached relative $\mathcal{O}(Q^4/M_{QCD}^4)$.

In the $f = 1$ sector, a nucleon interacts with low-energy probes. As the fermion in the NRQED example, the nucleon is static at LO because, having three-momentum of $\mathcal{O}(Q)$, it has a much smaller recoil energy of $\mathcal{O}(Q^2/m_N)$. The latter is accounted for at NLO, and relativistic corrections appear two orders higher. The classic process is pion-nucleon elastic scattering, details of which can be found in Refs. [47, 48]. LO consists of tree diagrams: an S-wave pion-nucleon seagull ("Weinberg-Tomozawa term") from the covariant derivative (4.39) of the nucleon, which is determined by f_π; and P-wave interactions via nucleon and Delta "pole diagrams" stemming from the pion-nucleon and pion-nucleon-Delta couplings of LECs g_A and h_A, respectively. By NDA, $g_A, h_A = \mathcal{O}(1)$, and indeed $g_A \simeq 1.3$ and $h_A \simeq 2.9$. At NLO we find not only the Galilean corrections to these couplings but also the effects of new seagulls. Two are associated with the shifts Δm_N and δm_N in nucleon mass, which gives the possibility of determining these parameters from scattering. Three other seagulls have undetermined coefficients $b_{1,2,3} = \mathcal{O}(1/M_{QCD})$. At N^{2}LO one-loop diagrams appear, including the leading contribution to the Delta width. At threshold the P-wave interactions vanish and the scattering length is purely isovector at LO, the classic Weinberg-Tomozawa result, extended to loop orders in the early 90s [49]. Other reactions can be studied along analogous lines [49].

As long as one considers $Q \ll m_\Delta - m_N$, the Δ field can be integrated out. The Lagrangian is formally the same as above, just without this field, but the LECs are in general different, because they now include Delta contributions. For example, the coefficients $b_{2,3}$ are replaced by larger LECs $c_{2,3} = \mathcal{O}(1/(m_\Delta - m_N))$. Delta effects are thus relegated to subleading orders, suppressed by powers of $Q/(m_\Delta - m_N)$. However, as the energy increases it is more efficient to keep the Delta in, and not consider $m_\Delta - m_N$ as large. If the energy is increased further, into the Delta resonance region, one finds a "kinematic" cancellation in an s-channel Delta propagator between energy E and $m_\Delta - m_N$, thus enhancing width effects. In a window $|E - (m_\Delta - m_N)| \ll \mathcal{O}(Q^3/M_{QCD}^2)$, the power counting (4.48) has to be modified [47, 50]. Delta width effects have to be resummed, allowing us to push ChPT beyond the Delta region. The Roper then becomes important in some waves and better be included as well [48].

ChPT has met with much success—for a recent review, see Ref. [51]—which emboldens us to press on to the sectors of Chiral EFT with $A \geq 2$ nucleons.

4.3.2.3 Nuclear Physics

As first noted by Weinberg [1], for $A \geq 2$ we face the same infrared enhancement we found in NRQED, which more generally takes place for heavy particles exchanging light quanta. Although the details are different, here this enhancement again leads to a breakdown of perturbation theory. This is a good thing, given that nuclei and we would not exist otherwise....

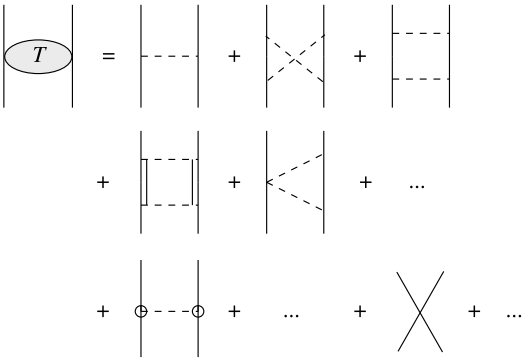

Fig. 4.3 Diagrams representing the T matrix for the elastic scattering of two nucleons in Chiral EFT. A nucleon (Delta) is represented by a (*double*) *solid line*, a pion by a *dashed line*. A *circle* at the vertex denotes an inverse power of M_{QCD}

As before, I start with two-body elastic scattering. Two nucleons can exchange photons as described in NRQED, but here I focus on the strong interactions mediated at long range by pion exchange, see Fig. 4.3. For the momenta, I follow the same notation as in Sect. 4.2.2.

Analogous to Eq. (4.25), the one-pion exchange (OPE) between two nucleons is

$$T_{1\pi} \simeq \left(\frac{g_A}{2f_\pi}\right)^2 \frac{\mathbf{q}^2}{\mathbf{q}^2 + m_\pi^2 - i\varepsilon} \boldsymbol{\sigma}_1 \cdot \hat{\mathbf{q}} \boldsymbol{\sigma}_2 \cdot \hat{\mathbf{q}} \overrightarrow{\tau}_1 \cdot \overrightarrow{\tau}_2 \big(1 + \mathcal{O}\big(Q^2/m_N^2\big)\big). \tag{4.49}$$

Since $g_A = \mathcal{O}(1)$, for $Q \sim m_\pi$ this term has magnitude $\mathcal{O}(1/f_\pi^2) = \mathcal{O}(4\pi/m_N M_{NN})$, where, for reasons that will become apparent soon, I introduced the quantity $M_{NN} \equiv 4\pi f_\pi^2/m_N = \mathcal{O}(f_\pi)$. Again as in NRQED, we can, and should later, consider corrections to OPE from higher derivatives at the vertices, but they are expected to be suppressed by $\mathcal{O}(Q^2/M_{QCD}^2)$ or higher.

If we look at the crossed-box two-pion-exchange (TPE) diagrams, we obtain an expression analogous to Eq. (4.26), but with the more complicated OPE substituted for photon exchange. We can count powers of $Q \sim m_\pi$ and 4π in the same way, that is, $Q^3/(4\pi)^2$ for the integration and Q^{-5} for the propagators, plus an extra Q/f_π for each vertex, to find an overall size $\mathcal{O}(Q^2/(4\pi f_\pi^2)^2)$, or a relative $\mathcal{O}(Q^2/(4\pi f_\pi)^2) = \mathcal{O}(Q^2/M_{QCD}^2)$ with respect to OPE. The same power counting applies to the stretched-box diagrams subsumed by the box diagram, and to diagrams originating in the Weinberg-Tomozawa seagull shown in Eq. (4.46). Substituting the Delta for the nucleon in intermediate states only adds modulating factors of $Q/(m_\Delta - m_N) = \mathcal{O}(1)$ in our counting. Thus, as in NRQED, we can consider these TPE diagrams as corrections to OPE, here starting at relative $\mathcal{O}(Q^2/M_{QCD}^2)$.

The true-box diagrams representing iterated OPE, on the other hand, have the same relative $\mathcal{O}(4\pi m_N/Q)$ enhancement as seen in Eq. (4.27): all nucleon energies are small and nucleon propagators are not static. Recoil, despite appearing only in $\mathscr{L}^{(1)}_{f=0,1}$ (4.47), cannot be treated as a perturbation. (This of course has nothing to do with relativistic corrections, although sometimes one sees a confusion in the literature, where the need for Galilean corrections is mistaken for a need for relativistic resummation.) The true-box diagrams have a size $\mathcal{O}(m_N Q/(4\pi f_\pi^4))$, or a

relative $\mathcal{O}(Q/M_{NN})$ with respect with OPE. More generally, iterating OPE n times gives a contribution of relative $\mathcal{O}(Q^n/M_{NN}^n)$. Qualitatively the amplitude is like a geometric series,

$$T^{(0)} \sim \frac{4\pi}{m_N M_{NN}} \left[1 - \mathcal{O}\left(\frac{Q}{M_{NN}} \right) \right]^{-1} . \tag{4.50}$$

Contrary to its NRQED counterpart (4.28), pion interactions are weak at low Q, but once $Q \sim M_{NN}$ bound states or resonances can be expected, with energies $|E| \sim M_{NN}^2/m_N$. Thus, by a reasoning entirely analogous to the one that gives the right atomic scales, we are led to identify the typical nuclear scale M_{nuc} with the low-energy scale $M_{NN} = \mathcal{O}(f_\pi)$. *Chiral-symmetry breaking*, in the form of a light pion with an interaction with strength set by $1/f_\pi$, *explains why nuclei are shallow from a QCD perspective*.

In addition to this qualitative insight, we see that in Chiral EFT the first aspect emerges of the traditional nuclear picture outlined in Sect. 4.2. Like NRQED, Chiral EFT reduces to nucleons interacting through a potential, which we define similarly and whose form we can derive. Since by construction we have no infrared enhancement in the potential, the ChPT power counting (4.48) applies to the corresponding pion-exchange diagrams. At LO, we find OPE. At NLO, or relative order $\mathcal{O}(Q/M_{QCD})$, there is nothing new because we are assuming P (and T) conservation. At N^{2}LO, we have corrections to OPE (including isospin violation) and the TPE diagrams discussed above, and at N^{3}LO, TPE diagrams with the seagull vertices from Eq. (4.46), in addition to isospin-breaking corrections. The isospin-symmetric potential up to this order was first derived in Refs. [3, 10], and rederived many times since (see discussion in Ref. [52]). As emphasized in Refs. [53, 54], this "chiral Van der Waals" potential has the qualitative features of heavier-meson exchange potentials, for example sigma+omega exchange in the isoscalar central channel. In Refs. [55, 56], the famous Nijmegen partial-wave analysis of two-nucleon ($2N$) data was redone with the chiral pion-exchange potential to N^{3}LO without Deltas as long-range input, instead of heavier-meson exchange. A slightly better fit laid to rest the longstanding prejudice that lack of explicit heavy meson exchange was a problem for EFT. At N^{4}LO, in addition to corrections to OPE and TPE, there is also three-pion exchange; the potential at this order has been derived in a *tour de force* in Ref. [57], and references therein. It seems unlikely that anything beyond this order will be needed. Note that in the literature sometimes relative $\mathcal{O}(Q^n/M_{QCD}^n)$, $n \geq 2$, is referred to as N^{n-1}LO instead of N^{n}LO as I do here.

We can go on and examine the implications of power counting for systems with $A \geq 3$ nucleons. Eq. (4.48) indeed provides the ordering of pion-exchange diagrams that generate an f-body force. For example, the leading three-nucleon ($3N$) force comes from tree diagrams with vertices from $\mathscr{L}^{(0)}$, and the next-to-leading component from tree diagrams with insertion of one vertex from $\mathscr{L}^{(1)}$. One can show that among the leading diagrams only TPE involving the Delta survives a cancellation against subleading terms in the OPE two-body force [8], resulting in the Fujita-Miyazawa potential as the dominant $3N$ force. The next-to-leading TPE diagrams in turn provide a chiral-corrected version of the Tucson-Melbourne (TM) potential,

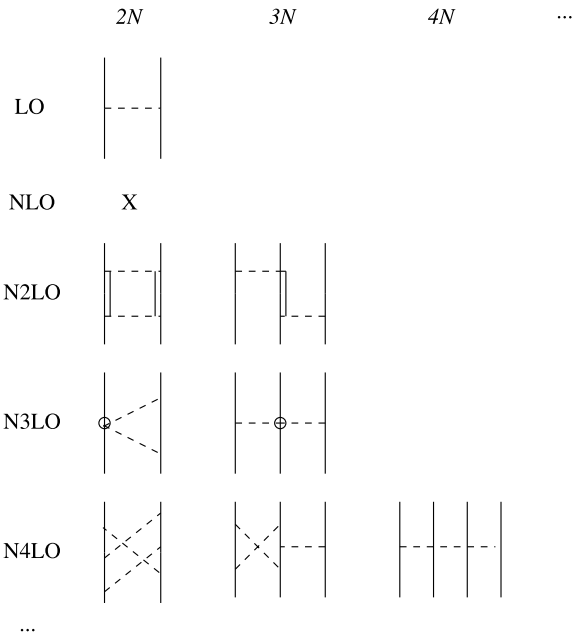

Fig. 4.4 Sample of diagrams representing the pion-range components of the isospin-symmetric part of the nuclear potential in Chiral EFT. N^{n}LO stands for relative $\mathcal{O}(Q^n/M_{QCD}^n)$. (Note that in the literature sometimes terms with $n \geq 2$ are referred to as N^{n-1}LO.) Notation as in Fig. 4.3

sometimes called the TM' potential [58, 59]. The leading long-range $4N$ potential has been derived as well [60, 61].

However, the relative ordering between potentials involving different numbers of nucleons is slightly more complicated. In the A-body system the A-body force connects all bodies while the $A-1$-body force, for example, leaves one of the bodies disconnected. Allowing for such disconnected diagrams in the power counting leads to an extra factor $-2C$, where C is the number of connected pieces, on the right-hand side of Eq. (4.48) [2]. We then recover the second aspect of the traditional nuclear picture: effects of the $2N$ potential are expected to be larger than those of the $3N$ potential, which in turn are expected to be larger than those of the $4N$ potential, and so on. The structure of the isospin-symmetric part of the long-range nuclear potential is shown schematically in Fig. 4.4.

Chiral EFT also provides a justification for the other two aspects of the traditional picture presented in Sect. 4.2. First, isospin is an accidental symmetry in Chiral EFT like spin symmetry in NRQED. Thus its violation is not represented by ε but at best by $\varepsilon Q/M_{QCD}$ [6]. The most important pieces of the isospin-violating potential can be obtained from the isospin-breaking terms in Eq. (4.47), and from the higher-index Lagrangians—see Ref. [62], and references therein. One finds that not only the isospin-symmetric potential tends to dominate, but also that charge independence tends to be larger than charge-symmetry breaking [9]. Second, by defining currents as the sum of diagrams with external probes that are free of infrared enhancement, we can likewise conclude that effects of one-nucleon currents are expected to be larger than those of $2N$ currents, which in turn are expected to be larger than those of $3N$ currents, and so on [5].

I have so far emphasized the long-range contributions from pions, but none of the qualitative conclusions change as long as we assume that LECs that account for short-range interactions among two or more nucleons obey NDA. In this case it is convenient to classify $\mathscr{L}_{f\geq 2}$ also according to the index (4.45),

$$\mathscr{L}_{f\geq 2} = \sum_{\Delta=0}^{\infty} \mathscr{L}_{f\geq 2}^{(\Delta)}. \tag{4.51}$$

The lowest-index terms have $f = 2$ and $d = 0$. Because of isospin, two nucleons can be found with total spin $s = 0, 1$ and we can now write two independent no-derivative interactions, corresponding to the two spin projectors (4.29):

$$\begin{aligned}\mathscr{L}_{f\geq 2}^{(0)} = &-\frac{C_{0(0)}}{4}(\bar{N}N\bar{N}N - \bar{N}\boldsymbol{\sigma}N\cdot\bar{N}\boldsymbol{\sigma}N)\\ &-\frac{C_{0(1)}}{4}(3\,\bar{N}N\bar{N}N + \bar{N}\boldsymbol{\sigma}N\cdot\bar{N}\boldsymbol{\sigma}N) + \cdots,\end{aligned} \tag{4.52}$$

with two LECs $C_{0(0,1)}$ and "…" standing for terms with Deltas. Using Fierz reordering, other isospin-symmetric forms can be written in terms of these. We can increase the index by one unit with an extra derivative or two more fermion fields,

$$\mathscr{L}_{f\geq 2}^{(1)} = \frac{D_0}{f_\pi}\bar{N}N\bar{N}\boldsymbol{\sigma}\overrightarrow{\tau}N\cdot\cdot\mathbf{D}\overrightarrow{\pi} - E_0\bar{N}N\bar{N}N\bar{N}N + \cdots, \tag{4.53}$$

where D_0 and E_0 are new LECs. Again, other forms can be reduced to these. For example, because of the Pauli principle, three nucleons at the same spacetime point can only have a total spin $s = 1/2$, so other six-nucleon operators can be rewritten in terms of E_0. Among the higher-index terms, I will also need

$$\begin{aligned}\mathscr{L}_{f\geq 2}^{(2)} = &-\frac{D_{2(0)}}{4}m_\pi^2(\bar{N}N\bar{N}N - \bar{N}\boldsymbol{\sigma}N\cdot\bar{N}\boldsymbol{\sigma}N)\left(1 - \frac{\overrightarrow{\pi}^2}{4f_\pi^2} + \cdots\right)\\ &-\frac{C_{2(0)}}{4}\left(\bar{N}N\bar{N}\mathscr{D}^2N - \bar{N}\boldsymbol{\sigma}N\cdot\bar{N}\boldsymbol{\sigma}\mathscr{D}^2N + \text{H.c.}\right)\\ &-\frac{C'_{2(1)}}{4}\left[3\,\bar{N}N(\mathscr{D}_i\bar{N})\mathscr{D}_iN + \bar{N}\boldsymbol{\sigma}N\cdot(\mathscr{D}_i\bar{N})\boldsymbol{\sigma}\mathscr{D}_iN + \text{H.c.}\right]\\ &+\cdots,\end{aligned} \tag{4.54}$$

where $D_{2(0)}$, $C_{2(0)}$, and $C'_{2(1)}$ are further LECs. The "…" now involve also other interactions with only nucleon fields, such as analogous terms for different spin and/or derivative combinations.

These short-range interactions are, of course, very important in quantitative applications of EFT. With the NDA assumption, we can use the index in Eq. (4.48) for the full potential, not only the pion-exchange diagrams shown in Fig. 4.4. The $C_{0(s)}$ terms appear already in the LO $2N$ potential, since $(C_{0(s)})_R =$

$M_{QCD}^2 C_{0(s)}/(4\pi)^2 = \mathcal{O}(1)$, or $C_{0(s)} = \mathcal{O}((4\pi)^2/M_{QCD}^2) = \mathcal{O}(4\pi/(m_N M_{NN}))$. These terms contribute to the two S-wave channels, ${}^1S_0$ and ${}^3S_1$ in the notation ${}^{2s+1}l_j$ where l and j are the orbital and total angular momenta, respectively. At N^{2}LO further contact interactions with two derivatives or two powers of the pion mass show up, suppressed by $\mathcal{O}((Q/M_{QCD})^2)$. For example, since by NDA $(C_{2(s)}^{(\prime)})_R = M_{QCD}^4 C_{2(s)}^{(\prime)}/(4\pi)^2 = \mathcal{O}(1)$ and $(D_{2(0)} m_\pi^2)_R = M_{QCD}^2 D_{2(0)} m_\pi^2/(4\pi)^2 = \mathcal{O}(\bar{m}_R)$, we have $C_{2(s)}^{(\prime)}, D_{2(0)} = \mathcal{O}(4\pi/(m_N M_{NN} \times M_{QCD}^2))$. These interactions provide (i) pion-mass- and momentum-dependent corrections in the S waves, such as $D_{2(0)}$ and $C_{2(0)}$, respectively; and (ii) short-range contributions to P waves, such as $C'_{2(1)}$. The pattern repeats at higher orders. Many of the corresponding LECs are necessary for the renormalization of the loops in the potential. The $2N$ potential then resembles some phenomenological potentials, such as AV18, where pion exchange is supplemented by a general short-range structure.

Likewise, the D_0 and E_0 terms come in the subleading $3N$ potential [8, 63]. While E_0 represents a purely short-range $3N$ effect, D_0 gives rise to a mixed-range force when the pion is attached to a third nucleon. In recent years this chiral $3N$ potential has been used in many *ab initio* nuclear calculations—see, *e.g.* Ref. [64]. For a review of chiral potentials under the assumption of NDA, including higher orders, see Ref. [16].

Following Weinberg's original suggestion [1], most calculations with these EFT-based potentials treat them in the same way as phenomenological potentials: once the form of the potential to the desired order has been derived, the appropriate dynamical equation—Lippmann-Schwinger, Schrödinger, or their few-body variants—is solved exactly (within numerical accuracy), and the unknown LECs fitted to data. After a promising start with the N^{3}LO $2N$ potential with Delta [7, 10], many years of efforts have now produced N^{4}LO $2N$ potentials without Delta that fit $2N$ data with an accuracy comparable to the best phenomenological potentials [16]. Adding the $3N$ force that appears at N^{3}LO gives a reasonable description of $A = 3, 4$ systems and beyond [64]. Still, remaining issues have led some to wait for a full N^{4}LO Deltaless potential, while others are rediscovering the Deltaful potential.

A number of processes with external probes have also been considered with Chiral EFT input, under the assumption of NDA for short-range multi-nucleon operators. They have in some cases led to results similar to earlier phenomenology, but in other cases they have given distinct, new predictions—such as, for example, the magnitude of threshold $\gamma d \to \pi^0 d$ [65] and the sign of the charge-symmetry-breaking asymmetry in $np \to d\pi^0$ [66].

But is NDA, inferred in perturbative calculations, valid for the LECs that appear in the non-perturbative, multi-nucleon sector of the EFT? And does it make sense to treat high-order corrections in the potential the same way as lowest order, instead of using perturbation theory as in NRQED? I explain next why *NO* is the right answer to both questions.

4.3.3 Renormalization of Singular Potentials and Power Counting

At the center of any EFT stands the issue of consistency, which of course is much more important than fitting data. Since EFT's model independence stems from an assumed integration over all higher-energy physics, its power counting has to yield approximate RG invariance at each order. In the case at hand, it is not obvious *a priori* that solving a dynamical equation with an NDA-based potential produces physical amplitudes free of cutoff dependence, even if the cutoff dependence of the potential has been removed. Solving a dynamical equation is just a means of accounting for reducible diagrams, which contain loops of a different type than those in the potential, but loops nevertheless. Whether such loops lead to cutoff dependence of the amplitude depends on the high-momentum, or equivalently small-distance, behavior of the potential. The problem is that an EFT-based potential gets more singular for vanishing radial distance, $r \to 0$, as the order increases.

Unfortunately, it is now known that a chiral potential based on NDA, as formulated so far, is not consistent with the RG. Despite their accuracy with respect to data, existing chiral potentials have to be replaced. Chiral potentials are just too singular, in the sense that they behave at the origin worse than r^{-2}, in both the pion-exchange and short-range components. In coordinate space, from Eq. (4.49), the LO OPE between two nucleons is, in spin-singlet and -triplet channels,

$$V_{1\pi,s=0} = \left(\frac{g_A}{2f_\pi}\right)^2 \overrightarrow{\tau}_1 \cdot \overrightarrow{\tau}_2 \left(\delta(\mathbf{r}) - \frac{m_\pi^2}{4\pi r} e^{-m_\pi r}\right) \tag{4.55}$$

$$V_{1\pi,s=1} = \left(\frac{g_A}{2f_\pi}\right)^2 \overrightarrow{\tau}_1 \cdot \overrightarrow{\tau}_2 \left[-\frac{1}{3}\left(\delta(\mathbf{r}) - \frac{m_\pi^2}{4\pi r} e^{-m_\pi r}\right) + \frac{1}{4\pi r^3}\left(1 + m_\pi r + \frac{(m_\pi r)^2}{3}\right) e^{-m_\pi r} \left\langle S_{12}(\hat{\mathbf{r}})\right\rangle\right], \tag{4.56}$$

where $\langle S_{12}(\hat{\mathbf{r}})\rangle = \langle (3\boldsymbol{\sigma}_1 \cdot \hat{\mathbf{r}} \boldsymbol{\sigma}_2 \cdot \hat{\mathbf{r}} - \boldsymbol{\sigma}_1 \cdot \boldsymbol{\sigma}_2)\rangle$ is the matrix element of the tensor operator. The tensor operator mixes waves of $l = j \pm 1$, where it has one positive and one negative eigenvalue, except for ${}^3P_0$ where it is diagonal with a negative eigenvalue. It also acts on states with $l = j$, where it has a positive eigenvalue. Considering the matrix elements of the isospin operator, the Yukawa part of $V_{1\pi}$ is attractive in isovector (isoscalar) channels for $s = 0$ ($s = 1$). The tensor part of $V_{1\pi,s=1}$ is attractive in some uncoupled waves like ${}^3P_0$ and ${}^3D_2$, and in one of the eigenchannels of each coupled wave. OPE is thus much more singular (and complicated!) than the Coulomb potential α/r in NRQED. At LO there are minimally also the (singular) $C_{0(s)}$ delta functions from Eq. (4.52), which can be combined with the delta functions in Eqs. (4.55) and (4.56). And the potential is more singular still at higher orders.

It has been known for a long time that attractive singular potentials require additional short-range parameters, and EFT provides just the tools, via renormalization, to make the solution of the Schrödinger equation well defined. The conclusion about

the bad RG behavior of NDA-based potentials is of course independent of the regularization procedure, so for illustration I will consider an intuitive regularization in coordinate space via a cutoff radius $R \equiv 1/\Lambda$. The long-range potential is unmodified for $r > R$, but for $r < R$ it is set to zero and a square well (and its derivatives) is taken instead. This short-range potential is a regularization of delta functions (and derivatives). Renormalization means that at each order the parameter(s) of the short-range potential can be found as functions of R in such a way as to keep low-energy observables R-independent, at least when R is much smaller than the distance scales of the long-range potential.

Since the complicated spin-isospin structure is not particularly relevant for renormalization, let me for simplicity consider a single uncoupled wave with a central potential

$$V(r) = -\frac{\alpha(R)}{2\mu R^2}\theta\left(1 - \frac{r}{R}\right) - \frac{\lambda}{2\mu r_0^2}\frac{f(r/r_0)}{(r/r_0)^n}, \tag{4.57}$$

where r_0 is a characteristic distance in the modulating regular function $f(r/r_0)$ such that $f(0) = 1$, λ is a dimensionless strength, n is an integer, and the dimensionless $\alpha(R)$ is a function of R. For the nuclear case with OPE, $\mu = m_N/2$, $r_0 = 1/m_\pi$, and $|\lambda| \sim m_\pi/M_{NN}$. In $s = 0$ channels, $n = 1$ and $f(x) = \exp(-x)$, while in $s = 1$ channels, $n = 3$ and $f(x)$ is slightly more complicated.

In order to solve this problem, one matches at $r = R$ the log-derivative of the solutions of the Schrödinger equation for the two regions $r < R$ and $r > R$. Let me focus first on $l = 0$, where at zero energy one obtains

$$\sqrt{\alpha(R)}\,\cot\sqrt{\alpha(R)} = F_n(\lambda, r_0, R), \tag{4.58}$$

with $F_n(\lambda, r_0, R)$ a complicated function obtained from the outside wavefunction. The issue is whether an $\alpha(R)$ can be found when $R \ll r_0$ such that the low-energy T matrix satisfies Eq. (4.16).

The case $n = 1$ might seem innocuous, as in this case the long-range part of the potential is *not* singular. Yet, the delta function is, and we find the first surprise here. In this case the potential is Coulombic for $R < r \ll r_0$, so the external wavefunction is given by a combination of regular and irregular Bessel functions. One finds [67]

$$F_1(\lambda, r_0, R) = -\lambda\frac{R}{r_0}\log\left(\frac{R}{R_\star}\right)\left[1 + \mathcal{O}(R/r_0)\right], \tag{4.59}$$

where $R_\star$ is a constant that determines the appropriate combination of external solutions for a given low-energy datum. The desired $\alpha(R)$ is

$$\alpha(R) = \left(k + \frac{1}{2}\right)^2\pi^2 + 2\lambda\frac{R}{r_0}\log\left(\frac{R}{R_\star}\right) + \mathcal{O}\left(R^2/r_0^2\right), \tag{4.60}$$

where k is an integer. One can then show that the amplitude at low (not necessarily zero) energies approaches cutoff independent results.

This is quite satisfactory, *except* for the fact that $\alpha(R)$ has to have a piece linear in $\lambda/r_0 \sim m_\pi^2/M_{NN}$. The interaction that it represents in the Chiral EFT Lagrangian is the chiral-symmetry breaking term with LEC $D_{2(0)}$ in Eq. (4.54). As it is obvious, this interaction is not the same as the $C_{0(s)}$ terms in Eq. (4.52): they give rise to different pionic interactions. By NDA $D_{2(0)}$ was supposed to be $\mathrm{N^2LO}$. Yet, we have just found that it is necessary at LO, if we take OPE as LO! Thus the magnitude of $D_{2(0)}$ is determined not by the high-energy scale M_{QCD} but instead by pion scales, and must be $D_{2(0)} = \mathcal{O}(4\pi/(m_N M_{NN}^3))$ instead. Note that this problem does not appear for $l > 0$, where one expects no delta function in LO, only the regular Yukawa potential.

Although this failure of NDA is of no particular consequence for the $2N$ problem itself, where only the combination $C_{0(0)} + D_{2(0)} m_\pi^2$ is measured, it should affect other processes like pion-nucleus scattering. Even more significantly, if NDA fails for this operator due to the non-perturbative nature of pion exchange, other operators might well suffer from the same problem. This was first pointed out in Ref. [68] and traced to the diagram where OPE is sandwiched between two contact interactions. The same authors [69] also noticed that thrice-iterated pion diagrams lead to cutoff dependence, but with two powers of momenta instead of two powers of the pion mass. Since in the NDA-based power counting two-derivative delta functions appear only at $\mathrm{N^2LO}$, just like $D_{2(0)}$, this suggests impending disaster—it could imply the need for infinite counterterms once the whole pion ladder is considered. These authors then proposed [69] that pions be treated in perturbation theory, that is, as an expansion in $|\lambda| \sim m_\pi/M_{NN}$. If this is done, LO contains only contact interactions $C_{0(s)}$, while OPE appears first as a single insertion at NLO together with $D_{2(0)}$ and the two-derivative S-wave contacts with LECs $C_{2(s)}$. More generally, a power counting can be devised that is consistent with the RG. (This power counting is, apart from the presence of pions, the same as the one for the Pionless EFT in the next lecture.) In $s = 0$ channels it seems this expansion does converge, although in ${}^1S_0$ only very slowly [67]. Unfortunately, for $s = 1$, where the tensor force can be attractive, the expansion fails already at $Q \sim f_\pi$ [70].

I am thus back to trying to make sense of the renormalization of non-perturbative OPE in $s = 1$ channels, where $n = 3$. When the potential is repulsive, one can solve the Schrödinger equation in the standard manner without any subtleties. For the interesting case $\lambda > 0$, on the other hand, the two outside solutions vanish as $r \to 0$ but oscillate indefinitely on the way there. There is no way to discard one; instead, we have again a combination of Bessel functions leading for $n \geq 2$ to [71]

$$F_n(\lambda, r_0, R) = \frac{n}{4} - \frac{\sqrt{\lambda}}{(R/r_0)^{n/2-1}} \tan\left(\frac{\sqrt{\lambda}}{(n/2-1)(R/r_0)^{n/2-1}} + \phi_n \right) \times \left[1 + \mathcal{O}\left((R/r_0)^{n/2-1}, R/r_0 \right) \right], \tag{4.61}$$

where ϕ_n is fixed by a given datum (the scattering length for $n > 3$). The corresponding $\alpha(R)$, found numerically, has a limit-cycle-like behavior: as R decreases, it decreases from $+\infty$ to $-\infty$ to start again in shorter and shorter cycles. Again, one finds that the scattering amplitude at finite energy is well behaved. We thus *can*

renormalize the $l = 0$ wave for a singular potential of this type with a single counterterm, despite the wild cutoff dependence of the diagrams in the corresponding perturbative series.

This bodes well for the LO chiral potential. Indeed, for $n = 3$ $\alpha(R)$ depends on $\lambda r_0 \sim 1/M_{NN}$, which is *in*dependent of m_π and thus represents a chiral-invariant counterterm like $C_{0(1)}$. One can show [67] that the coupled character of the ${}^3S_1$-${}^3D_1$ channels does not affect this conclusion. The NDA-based power counting seems to work in this case. Or does it?

In the final twist of this saga, hell breaks loose. What about channels with $l > 0$ where the singular potential is attractive? In these channels there is a repulsive centrifugal barrier $l(l+1)/r^2$, which dominates over the $-\lambda r_0/r^3$ potential at large distances. The situation gets reversed at short distances, where $-\lambda r_0/r^3$ again determines the wavefunction. Although the details of the matching change, one concludes that in *each* of these waves we need a new short-range parameter fixed by a low-energy datum. Clearly the NDA-based power counting does not provide any of these LECs at LO. If we insist in varying the cutoff in these waves, as we should, the phase shifts can be anything we want [72]. The simplest example is the ${}^3P_0$ wave where a bound state crosses threshold for a cutoff $\sim$1 GeV. The only way to fix [72] this problem is to take as LO an interaction like the $C'_{2(1)}$ term in Eq. (4.54), which if NDA were correct would only appear at N^{2}LO. Just like $D_{2(0)}$, we must have instead an enhancement, $C'_{2(1)} = \mathcal{O}(4\pi/(m_N M_{NN}^3))$. The situation is similar in the coupled ${}^3P_2$–${}^3F_2$ channels.

How many more LO interactions do we need? A simple estimate comes from the distance where the effective potential $-\lambda r_0/r^3 + l(l+1)/r^2$ is maximum, $r_m = 3\lambda r_0/(2l(l+1))$. When $r_m \lesssim 1/M_{QCD}$ the singular attractive potential is unimportant at large distances. The wavefunction oscillates only outside the region in which one expects the EFT to be valid. At the distances relevant to the EFT, the relatively smooth behavior of the wavefunction can be captured in perturbation theory. When one plugs in numbers, one finds that for $l \gtrsim 2$ pions are likely perturbative. This simple argument is corroborated by a more detailed calculation [73]. Thus, it seems that the correct LO consists of non-perturbative pions in S and P (and maybe D?) waves, with short-range interactions in the S and OPE-attractive P (and maybe D?) waves [72].

With the LO thus established, what about higher orders? It has been shown [74], in the context of a toy model, that as long as they are treated perturbatively (as in NRQED), the corrections in the amplitude can be renormalized with the short-range interactions given by a corrected NDA. In this corrected NDA, for a relative $(Q/M_{QCD})^n$ correction in the long-range potential, one includes short-range operators with n derivatives more than those appearing in LO. In other words, NDA applies once, but only once, we get to the perturbative corrections. For similar, but not identical, conclusions about the correct power counting from an RG-equation perspective, see Ref. [75].

A frequently asked question is, if the corrections are small enough to be perturbative, why can we not just treat them non-perturbatively, as done in existing versions of chiral potentials? The reason is simple: lack of counterterms. Take for example

a two-derivative contact interaction that appears in one insertion at N^2LO. In the same channel, two insertions will be in N^4LO, giving a highly singular contribution to the T matrix. This is however no problem as there will be at the same order an equally singular four-derivative contact interaction, which will provide the necessary counterterm. Only the sum of all N^4LO terms is cutoff independent and small. If I truncate at N^2LO (one needs to truncate somewhere...) but decide to iterate both LO and N^2LO, I automatically include diagrams with two (and many more!) insertions of the N^2LO operator without the required four-derivative counterterm. In general, my result will now be cutoff dependent, and there are likely regions of cutoff space where the "corrections" are no longer small. Not surprisingly, variations of the cutoff for truncations at N^3LO and N^4LO in Weinberg's scheme have been shown to lead to wild variation in the phase shifts [76, 77]. Existing chiral potentials can only fit data accurately in small windows in cutoff space. Note that not everybody thinks lack of RG invariance is important in this context [78].

The first calculations of the $2N$ system based on these new power-counting ideas give encouraging results [79–83], as one might have expected from the existence of more counterterms at each order than in NDA-based potentials. We can be optimistic about the development of a chiral potential that not only fits data well, but is also consistent with the RG. However, much remains to do to gauge the impact of these discoveries in systems with more nucleons and external probes.

4.3.4 Summary

A low-energy EFT of QCD has been constructed and used as input to *ab initio* methods to describe nuclear systems. Chiral symmetry plays an important role, in particular setting the scale for nuclear bound states. Several aspects of the traditional picture of nuclear physics emerge from the chiral potential, which additionally provides consistent few-body forces and currents, and systematic treatment of loop and isospin-breaking corrections. Unfortunately, though, the simplest power counting, based on naive dimensional analysis, is inconsistent with the renormalization group. A new, consistent power counting has been formulated, but is still mostly virgin territory.

4.4 Loosely Bound Systems

Chiral EFT provides a foundation for the physics of nuclei, at least when A is not too large. However, some nuclei are loosely bound in the natural binding energy scale of $\mathcal{O}(M_{nuc}^2/M_{QCD})$. The dynamics of these nuclei mostly takes place at distances large compared to $1/M_{nuc}$. We might expect new degrees of freedom and structures to emerge and, indeed, many loosely bound states display clusterization and other

phenomena like Borromean-type binding, where a system is bound even if its subsystems are not. In addition, loosely bound nuclei are important in an astrophysics context, sometimes at energies too low to achieve in the lab.

The relatively large distance scale means that fewer of the features of QCD, such as chiral symmetry, leave an imprint on the physics. On the upside, these systems share similarities with other loosely bound systems, where the underlying dynamics might be dominated by other EFTs than QCD, for example atomic systems where the underlying theory is NRQED. This universality is the overarching theme of this last lecture, where I first discuss how a low-momentum scale might arise, and then how two EFTs—Pionless and Halo/Cluster—describe nuclei at this scale.

4.4.1 Fine-Tuning

It has long been remarked that the deuteron is relatively large. From the deuteron binding energy $B_d \simeq 2.2$ MeV, an estimate for the deuteron binding momentum is $\aleph_1 \sim \sqrt{m_N B_d} \sim 45$ MeV, smaller than m_π by a factor of about 3. This means that the two nucleons are effectively at a distance three times larger than the range of the force, which prompted very early attempts by Bethe and Peierls, and others to describe deuteron physics with only schematic short-range potentials, such as a square well. The situation is even more dramatic for the ${}^1S_0$ virtual state, a structure in the T matrix to which we can associate a negative energy $-B_{d^*} \simeq -0.07$ MeV and thus a momentum $\aleph_0 \sim \sqrt{m_N B_{d^*}} \sim 8$ MeV, almost 20 times smaller than the pion mass.

For a generic short-range potential of range R, the two-body amplitude in the S wave can be written for $kR \ll 1$ in the form of the effective range expansion (ERE),

$$T_0(k) = \frac{2\pi}{\mu}\left[-\frac{1}{a_2} + \frac{r_2}{2}k^2 + \cdots - ik\right]^{-1}, \tag{4.62}$$

with a_2 and r_2 the scattering length and effective range parameter, and higher ERE terms not shown explicitly. If the effective range has a natural size $r_2 \sim R$, and the same is true of other ERE parameters, a shallow bound state of binding momentum $k = i\kappa$, $\kappa \sim 1/a_2$, is possible if $|a_2| \gg R$. This is the case of the $2N$ system, given that the effective ranges and other ERE parameters have natural sizes, for example $r_{2(1)} \simeq 1.75$ fm and $r_{2(0)} \simeq 2.8$ fm, but $a_{2(1)} \simeq 5.4$ fm and $a_{2(0)} \approx 20$ fm in the ${}^3S_1$ and ${}^1S_0$ channels, respectively, are much larger than $1/m_\pi$. Thus we are close to the unitarity limit defined by $a_2 \to \infty$ with other ERE parameters vanishing.

This situation suggests that the parameters of QCD are fine-tuned. Take as a very simple example a square well in the notation of Eq. (4.57), with $\lambda = 0$ and R not a cutoff but the physical scale associated with the range of the force. In that case one can find an analytic formula for the S-wave T matrix,

$$T_0(k) = i\left[1 - e^{-2ikR}\frac{\sqrt{\alpha + (kR)^2}\cot\sqrt{\alpha + (kR)^2} + ikR}{\sqrt{\alpha + (kR)^2}\cot\sqrt{\alpha + (kR)^2} - ikR}\right], \tag{4.63}$$

which takes the form (4.62) for $kR \ll 1$, with

$$a_2 = R\left(1 - \frac{\tan\sqrt{\alpha}}{\sqrt{\alpha}}\right), \qquad r_2 = R\left(1 - \frac{R}{\alpha a_2} - \frac{R^2}{3a_2^2}\right), \qquad \dots \tag{4.64}$$

For generic $\alpha = \mathcal{O}(1)$, $|a_2| \sim |r_2| \sim R$. However, if we dial α close to the critical value $\alpha_c \equiv [(2n+1)\pi/2]^2$ with n an integer, that is, if $|1 - \sqrt{\alpha/\alpha_c}| \ll 1$, then $R/|a_2| = \alpha_c|1 - \sqrt{\alpha/\alpha_c}| + \cdots \ll 1$, without changing the size of other ERE parameters significantly. By this fine-tuning a low momentum scale $\aleph \equiv |1 - \sqrt{\alpha/\alpha_c}|/R \ll 1/R$ appears in the system. Since there is a zero-energy pole in (4.63) at $\alpha = \alpha_c$, the fine-tuning means a shallow real or virtual bound state. For a real one, the wavefunction is normalizable, $\psi \propto \exp(-r/a_2)/r$, indicating a large size. This type of object is intrinsically quantum mechanical, since in classical physics bound-state sizes are limited by the range of the potential.

The details are different in the nuclear case where the LO potential consists of OPE plus contact interactions, instead of a simple square well. Still, at the physical pion mass the potential parameters must conspire to give the observed large scattering lengths. Now, all chiral-symmetric parameters are tied together by the non-perturbative QCD dynamics determined by the strong-coupling g. But the (current) quark masses, and thus the pion masses, can be considered largely independent of g in the SM. Therefore we can ask the question whether the fine-tuning can be undone by a variation in m_π. In Ref. [67] it was argued, based on a incomplete N^{2}LO analysis, that this might just be the case: the deuteron and virtual state can go unbound or bound with small variations of m_π. With some reasonable assumptions, the deuteron was found to have a more natural binding energy ~ 10 MeV in the chiral limit, and to become unbound at $m_{\pi,c} \simeq 200$ MeV, where the scattering length diverges. This analysis was later refined and compared with emerging full lattice QCD data, as described in Ref. [84]. Currently there is feverish activity in lattice QCD to calculate the binding energies in the $2N$ system (and other light nuclei) at various values of m_π (see Ref. [85] and references therein). Although there is no consensus yet, it seems that $m_{\pi,c}$ might actually be just below the physical pion mass. Either way, if this picture stands the test of lattice QCD, one can see the fine-tuning scale as $\aleph \equiv |1 - m_\pi/m_{\pi,c}|M_{nuc} \ll M_{nuc}$. The curve $a_2(m_\pi)$ [67] is in fact very similar to $a_2(B)$, where B is an external magnetic field, for atoms near a Feshbach resonance. Therefore it could very well be that we can think of QCD as near a Feshbach resonance in the quark masses.

There is no good explanation for this fine-tuning, yet. But we can exploit it by devising simpler EFTs that are valid only for momenta smaller than M_{nuc}, where even pion physics can be considered short-ranged.

4.4.2 Contact EFT

For $Q \sim \aleph \ll M_{nuc}$ (with $\aleph$ some average of $\aleph_{0,1}$), pions (and Deltas) can be integrated out: in few-nucleon systems, only nucleons are relevant degrees of freedom.

Chiral symmetry is badly broken and of no use. The most general Lagrangian with Lorentz and electromagnetic gauge invariance (and P and T symmetries) is a simplified version of what we had in the previous lecture:

$$\begin{aligned}\mathscr{L}_{piless} = \bar{N}\left(iD_0 + \frac{\mathbf{D}^2}{2m_N} - \frac{\delta m_N}{2}\tau_3\right)N - \frac{1}{4}F_{\mu\nu}F^{\mu\nu} \\ + \frac{e}{4m_N}\bar{N}\big[1+\kappa_0+(1+\kappa_1)\tau_3\big]\sigma_i N\tilde{F}^{0i} + \cdots \\ + \mathscr{L}_{f\geq 2}\end{aligned} \tag{4.65}$$

in the same notation as before. In the $f = 0, 1$ sectors the theory reduces to NRQED, so I will focus on $f \geq 2$,

$$\begin{aligned}\mathscr{L}_{f\geq 2} = &-\frac{C_{0(0)}}{4}(\bar{N}N\bar{N}N - \bar{N}\boldsymbol{\sigma}N\cdot\bar{N}\boldsymbol{\sigma}N) - \frac{C_{0(1)}}{4}(3\,\bar{N}N\bar{N}N + \bar{N}\boldsymbol{\sigma}N\cdot\bar{N}\boldsymbol{\sigma}N) \\ &- \frac{\delta C_{0(0)}}{4}\left(\bar{N}\frac{1+\tau_3}{2}N\bar{N}\frac{1+\tau_3}{2}N - \bar{N}\boldsymbol{\sigma}\frac{1+\tau_3}{2}N\cdot\bar{N}\boldsymbol{\sigma}\frac{1+\tau_3}{2}N\right) \\ &- E_0\bar{N}N\bar{N}N\bar{N}N \\ &- \frac{C_{2(0)}}{4}\big(\bar{N}N\bar{N}\mathbf{D}^2N - \bar{N}\boldsymbol{\sigma}N\cdot\bar{N}\boldsymbol{\sigma}\mathbf{D}^2N + \text{H.c.}\big) + \cdots,\end{aligned} \tag{4.66}$$

where only some representative interactions are shown, which include an isospin-breaking contact for protons with LEC $\delta C_{0(0)}$. Although I am repeating symbols for some the LECs, it should be kept in mind that they are not the same as in the Chiral EFT of the previous lecture: here they implicitly include pion physics that in Chiral EFT is kept explicit.

It has sometimes been found convenient to reformulate [86] the theory in terms not only of nucleons but also "dibaryon" (or, for atoms, "dimeron") auxiliary fields $\overrightarrow{S}$ and $\mathbf{T}$ with the quantum numbers of the two S-wave $2N$ channels, that is, spin (isospin) 0 (1) and 1 (0), respectively. In this case the Lagrangian (4.66) can be rewritten [87] as

$$\begin{aligned}\mathscr{L}_{f\geq 2} = &-\Delta_0\,\overline{\overrightarrow{S}}\cdot\left(1 + \frac{\delta\Delta_0}{\Delta_0}\frac{1+\tau_3}{2}\right)\overrightarrow{S} - \frac{g_0}{\sqrt{2}}[\overline{\overrightarrow{S}}\cdot\overrightarrow{P}_0 NN + \text{H.c.}] \\ &- \Delta_1\overline{\mathbf{T}}\cdot\mathbf{T} - \frac{g_1}{\sqrt{2}}[\overline{\mathbf{T}}\cdot\mathbf{P}_1 NN + \text{H.c.}] \\ &+ h\bar{N}\left\{g_0^2\overline{\overrightarrow{S}}\cdot\overrightarrow{\tau}\,\overrightarrow{S}\cdot\overrightarrow{\tau} + \frac{g_0 g_1}{3}[\overline{\mathbf{T}}\cdot\boldsymbol{\sigma}\,\overrightarrow{S}\cdot\overrightarrow{\tau} + \text{H.c.}]\right. \\ &\left.+ g_1^2\bar{N}\overline{\mathbf{T}}\cdot\boldsymbol{\sigma}\mathbf{T}\cdot\boldsymbol{\sigma}\right\}N + \sigma_0\,\overline{\overrightarrow{S}}\cdot\left(iD_0 + \frac{\mathbf{D}^2}{4m_N}\right)\overrightarrow{S} \\ &+ \sigma_1\bar{\mathbf{T}}\cdot\left(iD_0 + \frac{\mathbf{D}^2}{4m_N}\right)\mathbf{T} + \cdots\end{aligned} \tag{4.67}$$

where $\overrightarrow{P}_0 = \sigma_2 \overrightarrow{\tau}\tau_2/\sqrt{2}$ and $\mathbf{P}_1 = \tau_2 \boldsymbol{\sigma}\sigma_2/\sqrt{2}$ are the projectors onto the S-wave $2N$ channels of spins $s = 0, 1$, $\Delta_{0,1}$, $\delta\Delta_0$, $g_{0,1}$, and h are LECs—which can be thought of as the residual masses and mass splitting of the dibaryons, their couplings to two nucleons, and a dibaryon-nucleon interaction— and $\sigma_{0,1} = \pm 1$. Integrating out these auxiliary fields we regain Eq. (4.66) with certain relations between the LECs.

We can define the potential as before, so that amplitudes consist simply of iterations of the potential. But here the potential takes the particularly simple form of a sum of delta functions and their derivatives or, alternatively, of dibaryon propagation in the s channel. Either way, the potential contains no loops. All there is to do is to understand the ordering of the various terms, calculate the loops that appear in the iteration of the potential, and make sure observables are RG invariant.

4.4.2.1 The Two-Nucleon System

For a system with $|a_2| \gg |r_2| \sim R$, two-body physics at momenta $Q \sim \aleph \equiv 1/|a_2|$ can be described in a simple expansion in $R/|a_2| \ll 1$. Since effective range and other ERE terms should have natural size, in a first approximation only the non-derivative contact interactions should contribute [88].

The two-body amplitude in LO is particularly simple, being a sequence of potential insertions separated by box-like loops as in Eq. (4.27), where instead of Coulomb interactions we have a contact interaction—see Fig. 4.5. The two simplest diagrams are the single and once-iterated contact interaction, in each S-wave channel, respectively,

$$T_{1c} = -C_{0(s)} \tag{4.68}$$

and

$$\begin{aligned} T_{2c} &= -iC_{0(s)}^2 \int \frac{d^4l}{(2\pi)^4} \frac{1}{l^0 + p^0 - (\mathbf{l}+\mathbf{p})^2/2m_N + i\varepsilon} \\ &\quad \times \frac{1}{-l^0 + p^0 - (\mathbf{l}+\mathbf{p})^2/2m_N + i\varepsilon} \\ &= m_N C_{0(s)}^2 \int \frac{d^3l}{(2\pi)^3} \frac{1}{\mathbf{l}^2 - 2m_N p^0 - i\varepsilon} \\ &= \frac{m_N}{4\pi} C_{0(s)}^2 \left[\gamma_1 \Lambda + ik + \mathcal{O}\left(k^2/\Lambda\right)\right], \end{aligned} \tag{4.69}$$

where γ_1 is a constant that depends on the exact regulator used to make the loop integral well-defined ($\gamma_1 = 2/\pi$ for a sharp momentum cutoff, for example). The potentially dangerous dependence on a positive power of Λ can be absorbed in $C_{0(s)}(\Lambda)$ itself, while the $1/\Lambda$ terms can be taken care of by higher-derivative contacts. As in any (properly renormalized) EFT, the meaningful contribution of the loop is the term that is non-analytic in the energy $2p^0 = k^2/m_N$. We can see explicitly that an

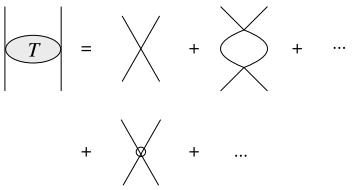

Fig. 4.5 Diagrams representing the T matrix for the elastic scattering of two nucleons in Pionless EFT. A nucleon is represented by a *solid line*. A *circle* at the vertex denotes an inverse power of M_{nuc}

intermediate state does indeed contribute $\mathcal{O}(m_N Q/(4\pi))$ to the amplitude as argued before. Each iteration therefore brings in a factor of $\mathcal{O}(m_N Q C_{0(s)}/(4\pi))$.

If $C_{0(s)} \equiv 4\pi/(m_N \aleph_s)$, then the LO two-body amplitude needs to be resummed for $Q \sim \aleph_s$, as we have done schematically before in Eqs. (4.28) and (4.50):

$$T^{(0)} \sim \frac{4\pi}{m_N \aleph_s}\left[1 - \mathcal{O}\left(\frac{Q}{\aleph_s}\right)\right]^{-1}. \tag{4.70}$$

But here we can be more explicit because, contrary to the earlier cases, the series is an exact geometric series:

$$T^{(0)} = \frac{4\pi}{m_N}\left[-\left(\frac{4\pi}{m_N C_{0(s)}} + \gamma_1 \Lambda\right) - ik\right]^{-1}\left[1 + \mathcal{O}\left(\frac{k}{\Lambda}\right)\right]. \tag{4.71}$$

Comparison with Eq. (4.62) shows that we recover the ERE in LO, with the cutoff-independent combination $C^R_{0(s)} \equiv C_{0(s)}(\Lambda)/(1 + m_N \gamma_1 \Lambda C_{0(s)}(\Lambda)/4\pi) = 4\pi a_{2(s)}/m_N$ capturing the physics of the large scattering length. The amplitude has a pole at imaginary momentum $k = i\kappa_s = i/a_{2(s)}$, which represents a real (virtual) bound state for $a_{2(s)} > 0$ (<0) with binding energy $B_{2(s)} = 1/(m_N a^2_{2(s)})$.

Thus the fine-tuning that generates a shallow S-wave bound state can be accounted for if $C_{0(s)}$ depends on the anomalously low scale $\aleph_s$. We can consider corrections that account for natural ERE parameters if the LECs of derivative operators scale with $\aleph_s$ and M_{nuc} in a particular way. The $\aleph_s$ enhancement depends on whether the LEC contributes to the S-wave. For example, $C_{2(s)} \sim 4\pi/(m_N M_{nuc} \aleph_s^2)$ gives rise to a relative correction $\mathcal{O}(Q^2/(M_{nuc}\aleph))$ in Eq. (4.71), which incorporates physics of an effective range $r_2 \sim 1/M_{nuc}$. Similar scalings apply to higher S-wave parameters, but not in other waves, where no shallow bound states exist. Thus, for example, $C'_{2(s)} \sim 4\pi/(m_N M^3_{nuc})$ gives the leading P-wave contribution to the amplitude at relative $\mathcal{O}(Q^3/M^3_{nuc})$. Higher waves appear at even higher orders. For more details, see Refs. [69, 89].

Note that, as in NRQED and Chiral EFT, the corrections in Eq. (4.71) should in principle be treated in distorted-wave perturbation theory, when RG invariance can be maintained. In the particular case of the dominant correction, $C_{2(s)}$, at NLO we consider just one insertion of its vertex, and any number of $C_{2(0)}$ vertices. At N^{2}LO we need two insertions, with one from the four-derivative interaction with

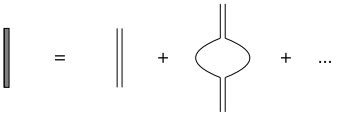

Fig. 4.6 Diagrams representing the reduced $\tilde{T}$ matrix for the elastic scattering of two nucleons in Pionless EFT. A nucleon is represented by a *solid line*, a dibaryon by a *double solid line*

LEC $C_{4(0)}$. Actually, the contributions from $C_{2(s)}$ *can* be resummed to the form (4.62) without destroying RG invariance, but only as long as $r_{2(s)} \leq 0$ [90], a form of the so-called Wigner bound. Since $r_{2(s)} > 0$ in the $2N$ case, one should indeed refrain from deviating from perturbation theory.

There is not much difficulty in adding Coulomb effects. As we have seen in NRQED, Coulomb becomes non-perturbative for $Q \lesssim \alpha m_N \sim 5$ MeV. This is not too far from the ${}^1S_0$ virtual bound state, that is, Coulomb effects $\mathcal{O}(4\pi\alpha/Q^2)$ become comparable to $C_{0(0)} = 4\pi/m_N \aleph_0$ for $Q^2 \lesssim \alpha m_N \aleph_0 \sim \aleph_0^2$. In the two-proton system, for such low momentum one needs to account for Coulomb in addition to a contact interaction at LO, which introduces new cutoff dependence. We therefore need to consider the additional contact interaction $\delta C_{0(0)}$, which is isospin breaking, to absorb this cutoff effect [91]. Since $\delta C_{0(0)}$ needs to be fitted to the pp scattering length, isospin breaking cannot be predicted at this order. Fortunately, at higher energies Coulomb and other electromagnetic interactions can be treated in perturbation theory.

We can recast these statements in the dibaryon formulation, where the dibaryon residual masses are taken to be fine-tuned, $\Delta_{0,1} \sim \aleph_{0,1}$, while the coupling constants are taken as natural-sized, for example $g_{0,1}^2 \sim 4\pi/m_N$. The dibaryons can be thought of as "bare" real and virtual bound-state fields, although this implies nothing about their composite nature. The S-wave $2N$ amplitudes are just the couplings of two nucleons to dibaryon propagators that are "dressed" by $2N$ loops. In LO only the dibaryon residual mass is needed in addition to the two-nucleon/dibaryon coupling. For the strong-interacting sector we can write

$$T = g_s^2 \tilde{T}, \tag{4.72}$$

with the reduced T matrix $\tilde{T}$ being the sum of successive bare dibaryon propagators depicted in Fig. 4.6,

$$\tilde{T}_{1d} + \tilde{T}_{2d} + \cdots = \frac{4\pi}{m_N g_s^2}\left[\left(\frac{4\pi\,\Delta_s}{m_N g_s^2} - \gamma_1 \Lambda\right) - ik\right]^{-1} \times \left[1 + \mathcal{O}\left(\frac{k}{\Lambda}\right)\right], \tag{4.73}$$

from which we see that renormalizability is achieved by absorbing the Λ dependence in Δ_s/g_s^2. Coulomb can be included just like above, requiring a renormalization of $\delta\Delta_0$. Dibaryon kinetic terms generate effective ranges at NLO, but these kinetic terms have signs $\sigma_{0,1}$ given by the sign of $-r_{2(0,1)}$. Since $r_{2(s)} > 0$, $\sigma_s < 0$ and the bare dibaryons are ghosts. However, their character changes when they get dressed, and the $2N$ amplitude has no pathology.

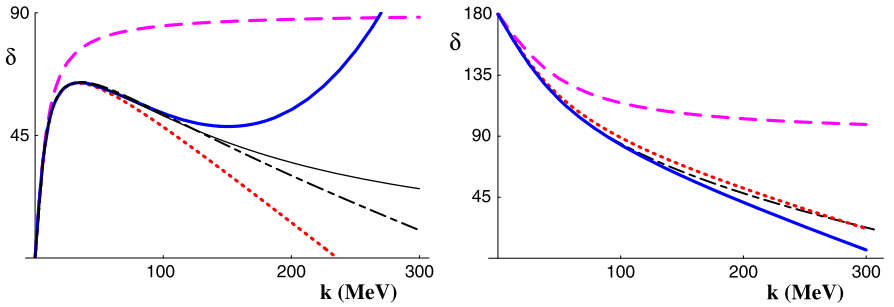

Fig. 4.7 The ${}^1S_0$ (*left*) and ${}^3S_1$ (*right*) $2N$ phase shifts (in degrees) as functions of the center-of–mass momentum (in MeV). The *dot-dashed lines* represent the Nijmegen phase-shift analysis [94]. *Left*: the *dashed*, *dotted*, and *thick solid lines* show the Pionless EFT results at LO, $\mathrm{N^2LO}$, and $\mathrm{N^4LO}$, respectively, while the *thin solid line* shows the ERE. *Right*: the *dashed*, *dotted*, and *thick solid lines* show the Pionless EFT results at LO, NLO, and $\mathrm{N^2LO}$, respectively. From Refs. [12, 92], courtesy of M. Savage

This approach, in either formulation, has been shown to give a very clear path to analyze low-energy reactions involving two nucleons systematically [13]. It is a field-theoretical generalization of the ERE. The resulting $2N$ phase shifts converge to empirical values for $Q \lesssim M_{nuc}$, as shown for the S waves in Fig. 4.7 [12, 92]. Deuteron properties come out well; for example the deuteron binding energy is found to be $B_d = 1.9$ MeV in NLO, to be compared with the experimental value of 2.2 MeV. More generally, this EFT can be applied to any system with $|a_2| \gg |r_2|$, for example bosonic or fermionic atoms near a Feshbach resonance [93].

4.4.2.2 The Three-Nucleon System

The $3N$ system proves to be much more interesting, since here the EFT is not just the ERE. There is no symmetry to forbid three-body forces like the E_0 term in Eq. (4.66) or the h term in Eq. (4.67). As always in any EFT, the question is just at what order these novel effects appear. If NDA were any guide, one would expect them at relatively high orders since their canonical dimensions are high. However, we are dealing with a fine-tuned situation, and surprises are in stock.

For definiteness, let me consider neutron-deuteron (nd) scattering in the dibaryon formulation, see Fig. 4.8. The simplest diagram consists of the transfer of one nucleon from the dibaryon to the third nucleon, and it is $\mathcal{O}(m_N g_s^2/Q^2)$. A transfer back adds another $m_N g_s^2/Q^2$ multiplied by a factor $Q^3/(4\pi)$ from the loop and a $1/Q$ from the intermediate, dressed dibaryon, so it is of relative $\mathcal{O}(m_N g_s^2/4\pi) = \mathcal{O}(1)$. Thus, power counting says that in LO one has to sum all nucleon exchanges between the dimeron and the third nucleon, resulting [88] in an integral equation for the T matrix known as the Skorniakov–Ter-Martirosian equation. As always, corrections can be treated in perturbation theory.

The behavior of this T matrix at large momentum turns out to depend sensitively on the strength of the kernel of the integral equation, which in turn depends on

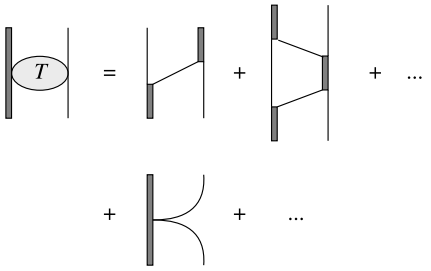

Fig. 4.8 Diagrams representing the T matrix for the elastic scattering of a neutron on a deuteron in Pionless EFT. Notation as in Fig. 4.6

the spins of particle and dimer. For a two-state fermion instead of a nucleon, when the dimer has $s = 0$, the amplitude falls fast at large momenta and the solution of Skorniakov–Ter-Martirosian equation is RG invariant, consistent with three-body forces appearing only at high orders. The same is true for nucleons in all but the $S_{1/2}$ wave, and very accurate results for nd scattering follow from parameters fully determined in $2N$ scattering [88, 95]. For example, for the $S_{3/2}$ phase shift shown in Fig. 4.9 excellent agreement with data is achieved already at $\mathrm{N^2LO}$. In particular, the scattering length is postdicted as $a_{3/2} = 6.33 \pm 0.10$ fm, to be compared to the experimental value, 6.35 ± 0.02 fm. This example shows that Pionless EFT enables nearly QED-quality nuclear physics.

On the other hand, for three bosonic particles or for nucleons in the $S_{1/2}$ wave of Nd scattering, the amplitude obtained from nucleon exchange alone has a very peculiar Λ dependence, proportional to $\cos(\ln \Lambda)$. A bound state of energy $\mathcal{O}(\Lambda^2/m_N)$ is in the spectrum, representing the well-known "Thomas collapse" of the ground state as $\Lambda \to \infty$. RG invariance can only be achieved if three-body interactions are enhanced by $\aleph^{-2}$ [96, 97]. A single non-derivative three-body interaction appears at LO, providing saturation to avoid the collapse. Higher-derivative interactions are smaller by powers of Q/M_{nuc}, and in fact to NLO there is only one parameter not fixed by $2N$ observables: the coefficient of the three-body force, h (or equivalently E_0). As a consequence, to this order three-body observables are correlated through this one parameter. This explains [87], in particular, why results obtained from $2N$ models cluster around a "Phillips line" in the plane generated by all possible values of the $S_{1/2}$ Nd scattering length $a_{1/2}$ and the triton binding energy B_t: the off-shell differences among $2N$ models are essentially captured by one parameter. Any point on the EFT line fixes the LO $3N$ parameter, which, as a function of Λ, displays an unusual, limit-cycle behavior [96]. If we use as input the $a_{1/2}$ experimental value, we find $B_t = 8.54$ MeV at NLO [98], to be compared with the experimental value of 8.48 MeV. The resulting energy dependence of $S_{1/2}$ Nd scattering also comes out very well, as shown in Fig. 4.9.

The limit cycle in the three-body force reflects a residual, approximate discrete scale invariance. At unitarity, the LO two-body T matrix is scale invariant in the limit $\Lambda \to \infty$. The only bound state is at zero energy. The regularization and renormalization of the three-body problem breaks scale invariance, except for the discrete scale invariance that survives as the cutoff takes values that are multiple of a value determined by the three-body datum. A consequence is that a geometric spectrum

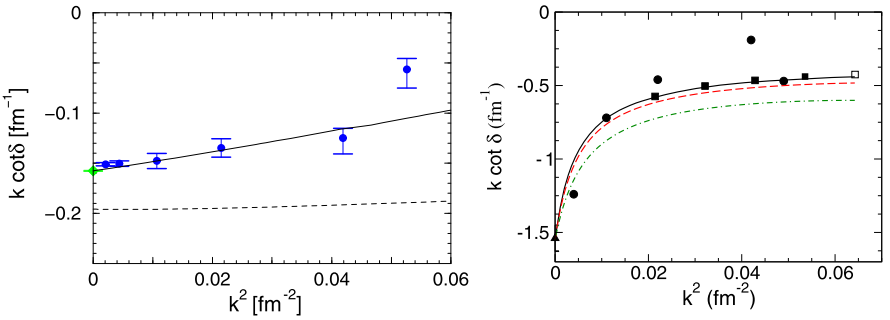

Fig. 4.9 The $S_{3/2}$ (*left*) and $S_{1/2}$ (*right*) Nd K^{-1} matrices (in fm^{-1}) as function of the square of the center-of-mass momentum (in fm^{-2}). *Dots* represent a cold-neutron measurement [99] and a phase-shift analysis [100, 101]. *Left*: *dashed* and *solid lines* show the Pionless EFT results at LO and $\mathrm{N^2LO}$, respectively. *Right*: *dot-dashed*, *dashed* and *solid lines* show the Pionless EFT results at LO, NLO, and $\mathrm{N^2LO}$, respectively, while the *squares* come from a phenomenological potential model [102]. From Refs. [95, 103], courtesy of H.-W. Hammer and L. Platter

of bound states appears, the famous Efimov effect. For large but finite scattering length and non-zero ERE parameters, scale invariance is only approximate to start with, and only bound states with binding energies $\lesssim 1/(2\mu R^2)$ are within the EFT.

Including Coulomb interactions in $3N$ calculations is a bit challenging, but it has been done (see Ref. [104] and references there in). Interactions with external photons, such as the triton electromagnetic form factor [105], are also beginning to be investigated. For a recent example of application to cold atoms, see Ref. [106]

4.4.2.3 The Four-Nucleon System and Beyond

I can proceed in a similar way to larger systems. Faced with the appearance of a $3N$ force at LO, an obvious question is whether other few-body forces are also leading. A hand-waving argument suggests they are not. The two-body system is made stable in Pionless EFT by a balance between kinetic repulsion and potential attraction. As we go to the three-body system, the number of pairs grows faster than the number of particles, leading to a collapse unless an effectively repulsive three-body force exists. As we add a fourth body, the number of triplets increases faster than doublets, and no instability and dramatic cutoff dependence should arise. Although a four-body force without derivatives exists, it might not be enhanced by inverse powers of $\aleph$. With four spin-isospin states, we cannot construct a five- or more-nucleon contact force without derivatives, so they are likely not to be LO either.

Since by this argument stability comes from a balance between two-body attraction and three-body repulsion, one expects properties of larger systems, such as four-body and nuclear-matter binding energies (if within Pionless EFT), to scale approximately with the LO three-body parameter. This has been shown to be true for the four-boson binding energy, at least over a limited Λ range [107]. In the $4N$

system one observes the Tjon line, which is the analog of the Phillips line, but for the alpha-particle binding energy B_α instead of the $S_{1/2}$ Nd scattering length $a_{1/2}$. This line is reproduced in Pionless EFT [108]. The LO EFT line depends a bit on which $2N$ parameters are used as input, but in any case it is close to the experimental point: at the correct B_t one finds B_α between 26.9 and 29.5 MeV, to be compared to the experimental value of 28.3 MeV. This agreement suggests that the EFT is converging for the alpha particle. An NLO calculation [109] seems to support this conclusion.

In the region $M_{nuc} \gg Q \gg \aleph$ the $2N$ T matrix has an approximate $SU(4)$ symmetry in spin-isospin space [110]. Since the LO $3N$ force is also $SU(4)$ symmetric [87], Pionless EFT provides a rationale for the emergence of Wigner's supermultiplet symmetry in nuclei.

However, a crucial question is how far we can go in A before pions can no longer be considered short-ranged. After all, binding energies per nucleon, and thus binding momenta, increase throughout the light-nuclear region as the number of nucleons increases. An answer to this question can only be provided by explicit calculation.

Because the continuum methods used so far for $A \leq 4$ tend to become unpractical quickly, one is led to introduce an explicit infrared (IR) momentum regulator or cutoff λ so as to discretize the set one-body states. One can think of $1/\lambda^3$ as providing an effective volume to which the system is confined, just as the inverse UV regulator, $1/\Lambda$, can be thought of as a minimum accessible length scale. These two regulators define the "model space" where the EFT is solved. At the end of the calculation, we need to take the limit of a large model space, $\lambda \ll Q \ll \Lambda$.

In this context, two such IR regulators have been proposed and are being actively pursued. The first [111] borrows from lattice QCD: we define the EFT at N^3 lattice points separated by a spacing $a \sim 1/\Lambda$, which make a cubic volume with sides of length $L = Na \sim 1/\lambda$. The second [112] borrows instead from an existing nuclear-structure method, the No-Core Shell Model (NCSM): the EFT is solved in a harmonic-oscillator well of frequency $\omega \sim \lambda^2/m_N$, with a maximum number of shells $2n + l \leq N_{max} \sim \Lambda^2/(m_N\omega)$—where n (l) denotes the radial (angular-momentum) quantum number—above the minimum configuration.

The limitation to an effectively finite volume poses the challenge of how to relate the LECs to observables. At LO the three LECs can be fitted to the binding energies of the lightest nuclei (deuteron, triton, alpha particle), with other binding energies being predictions (or postdictions). For example, using the NCSM method, one finds [112] for the alpha-particle excited state an excitation energy $E_{\alpha^*} = 18.5$ MeV, in remarkable (for LO) agreement with the experimental value 20.2 MeV, while for the ^{6}Li ground state $B_{^6\mathrm{Li}} = 23$ MeV to be compared to the experimental result, 32 MeV, in line with an expansion parameter $|r_2|/|a_2| \sim 1/3$. However, the growth in number of LECs with order demands the more abundant scattering data as input. Fortunately, for both methods we can related the energy levels in the model space to $2N$ scattering parameters [113, 114]. Thus, the $2N$ LECs can be fitted to $2N$ levels and, with just a few few-body inputs, predictions made for systems with larger number of particles.

Just as before, such a framework can be applied with simplifications also to cold atoms, see for example Ref. [115]. And these methods are being generalized to Chiral EFT—for reviews and more details, see Refs. [116, 117]. But these new ideas can also be used with more phenomenological input. The generic idea of using λ and Λ to extrapolate to larger model spaces, for example, is useful in calculations with phenomenological nuclear potentials [118, 119]. Conversely, other *ab initio* methods could be brought to bear on Pionless EFT. While Chiral EFT is the ultimate goal, because of its simplicity Pionless EFT plays an important role in providing a paradigm for the development of nuclear EFTs.

4.4.3 Halo/Cluster EFT

Pionless EFT simplifies the treatment of light nuclei, but its application to larger nuclei—even with a powerful *ab initio* method such as the NCSM—still faces difficult computational challenges. One would like to devise further simplifications in order to extend EFTs to even larger nuclei.

One might, in particular, wonder about the implications of the existence of the fine-tuned scale $\aleph$. While we expect the typical energy per nucleon to be $\mathcal{O}(M_{nuc}^2/m_N)$, there are some nuclear states with energies closer to $\mathcal{O}(\aleph^2/m_N)$. This is, in fact, the case of light nuclei, which, as we have just seen, seem to be within the regime of Pionless EFT. But this also happens in two more general classes of states: "halo" and "cluster" nuclei, in which one or more clusters of nucleons ("cores") with the structure of typical nuclei are surrounded by loosely bound ("halo") nucleons. Because of saturation, the radius of a typical cluster with A_c nucleons should be $R_c \sim A_c^{1/3}/M_{nuc} \equiv 1/M_c$. As long as $\aleph \ll M_c$, we can treat cores as effective degrees of freedom, thus generalizing Pionless EFT, where $A_c = 1$, to Halo/Cluster EFT [120].

These classes of systems exhibit shallow S-matrix poles, either on the imaginary axis (bound states) or in the lower half of the complex momentum plane (resonances). Many nuclei display, or are good candidates to display, halo/cluster structure with various types of cores. The simplest and perhaps most clear-cut examples involve alpha-particle cores, for which the excitation energy $E_{\rm core} \simeq 20$ MeV. While ^{5}He is not bound, the total cross section for neutron-alpha ($n\alpha$) scattering has a prominent bump at $E_{\rm halo} \sim 1$ MeV, interpreted as a shallow $P_{3/2}$ resonance. To describe scattering at such low energy, a two-body $\alpha + n$ approach should suffice. ^{6}He is bound, but the removal energy for two neutrons from ^{6}He is again $E_{\rm halo} \simeq 1$ MeV, making this a three-body, $\alpha + n + n$ halo nucleus. Similarly, ^{8}Be is not bound but $\alpha\alpha$ scattering shows an S_0 resonance at $E_{\rm halo} \simeq 0.1$ MeV. And both ^{9}Be and ^{12}C exhibit states near three-body thresholds, respectively $\alpha + \alpha + n$ and $\alpha + \alpha + \alpha$—the latter being the famous Hoyle state that plays an important role in the formation of C and O, and thus you and me, in the universe. Then we can consider also structures with protons, *e.g.* ^{5}Li as $\alpha + p$. For a compilation of data on these and some other halo/cluster states (and much more), see Ref. [121].

In Halo/Cluster EFT we thus consider explicitly a field for the core, for example a scalar field α for the α core of mass m_α:

$$\mathscr{L}_{\rm halo} = \bar{N}\left(iD_0 + \frac{\mathbf{D}^2}{2m_N} - \frac{\delta m_N}{2}\tau_3\right)N + \bar{\alpha}\left(iD_0 + \frac{\mathbf{D}^2}{2m_\alpha}\right)\alpha - \frac{1}{4}F_{\mu\nu}F^{\mu\nu} + \cdots + \mathscr{L}_{\geq 2}. \tag{4.74}$$

It is again extremely convenient to express $\mathscr{L}_{\geq 2}$ using dimeron fields, in this case a spin-3/2, isospin-1/2 field T_3 and a scalar, isoscalar ϕ for the ^{5}Li/^{5}He and ^{8}Be ground states, respectively:

$$\begin{aligned}\mathscr{L}_{\geq 2} = {} & \bar{T}_3\left[\sigma_3\left(iD_0 + \frac{\mathbf{D}^2}{2(m_N+m_\alpha)}\right) - \Delta_3\left(1 + \frac{\delta\Delta_3}{\Delta_3}\frac{1+\tau_3}{2}\right)\right]T_3 \\ & + \bar{\phi}\left[\sigma_0\left(iD_0 + \frac{\mathbf{D}^2}{4m_\alpha}\right) - \Delta_0\right]\phi + \frac{g_0}{\sqrt{2}}[\bar{\phi}\alpha\alpha + \text{H.c.}] \\ & + \frac{g_3}{\sqrt{2}}\left[\bar{T}_3\left(1 + \frac{\delta g_3}{g_3}\frac{1+\tau_3}{2}\right)\mathbf{S}\cdot(\alpha\mathbf{D}N + N\mathbf{D}\alpha) + \text{H.c.}\right] \\ & + h_3\bar{T}_3T_3(\overline{\mathbf{D}N})\cdot\mathbf{D}N + \cdots,\end{aligned} \tag{4.75}$$

where $\mathbf{S}$ is again the spin transition matrix, $\Delta_{0,3}$, $\delta\Delta_3$, $g_{0,3}$, δg_3, and h_3 are the most important LECs, and $\sigma_{0,3}$ are signs. This Lagrangian has a form similar to Eq. (4.67), except for the spin/isospin differences and the P-wave coupling of the ^{5}He/^{5}Li dimeron.

Similar Lagrangians can be written for other core types. If the core has a small number of low-lying excited states, they can be included as extra fields just like the Delta in Chiral EFT. The main drawback of Halo/Cluster EFT is the relatively large number of undetermined LECs, as different cores demand different LECs. As in other EFTs, one would like to eventually determine the LECs by matching low-energy amplitudes to *ab initio* calculations based on Pionless or Chiral EFTs. In the meantime they can be fitted to data.

4.4.3.1 Two-Body Systems

As with Pionless EFT, the first step is to determine the two-body LECs. Were we looking at a core-nucleon system that supports a shallow S-wave bound state, things here would be very similar to the $2N$ case. But many of the two-body systems of interest in Halo/Cluster EFT, and in particular $N\alpha$ and $\alpha\alpha$, have a shallow resonance instead of a bound state. The different pole structure requires a different power counting than in the $2N$ system. In this case the T matrix will be made out of dimeron propagators connected by two-particle bubbles just as before. But the required two-pole structure arises if both the kinetic and residual-mass terms in the dimeron propagators are of similar size.

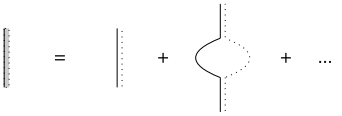

Fig. 4.10 Diagrams representing the reduced $\tilde{T}$ matrix for the elastic scattering of a nucleon on an alpha particle in Halo/Cluster EFT. A nucleon (alpha particle) is represented by a *solid* (*dotted*) *line*, and a dibaryon by a *double solid/dotted line*

The particular case of a narrow resonance, $\kappa_I \ll \kappa_R$, requires a single fine-tuning in the dibaryon mass [122]. For $N\alpha$, $\Delta_3 \sim \aleph^2/\mu_{3N}$, where $\mu_{3N} = m_N m_\alpha/(m_N + m_\alpha)$ is the $N\alpha$ reduced mass, while other parameters do not depend on $\aleph$, for example $g_3^2 \sim 2\pi/(\mu_{3N}^2 M_c)$. For simplicity, let me focus on $n\alpha$, Coulomb corrections being necessary for $p\alpha$. The T matrix in the $P_{3/2}$ channel can be written as [120]

$$T = \frac{g_3^2 k^2}{3}(2\cos\theta + i\sin\theta\boldsymbol{\sigma}\cdot\hat{\mathbf{n}})\tilde{T}, \tag{4.76}$$

in terms of $\mathbf{n} = \mathbf{p}\times\mathbf{p}'/|\mathbf{p}\times\mathbf{p}'|$, the scattering angle θ, and the reduced $\tilde{T}$ matrix shown in Fig. 4.10. The contribution from a single dibaryon propagator is

$$\tilde{T}_{1d} = \frac{1}{\Delta_3 - \sigma_3 k^2/(2\mu_{3n})}, \tag{4.77}$$

which is the analog of Eq. (4.68) in Pionless EFT. For $Q \sim \aleph$, this is $\mathcal{O}(\mu_{3N}/\aleph^2)$. For the once-iterated dibaryon propagator, the intermediate bubble is similar to Eq. (4.69), except for the presence of two extra momenta in the numerator inside the integral, which is therefore more sensitive to the cutoff:

$$\tilde{T}_{2d} = \frac{\mu_{3n} g_3^2}{6\pi}\tilde{T}_{1d}^2\left[\gamma_3\Lambda^3 + \gamma_1\Lambda k^2 + ik^3 + \mathcal{O}\left(\frac{k^4}{\Lambda}\right)\right], \tag{4.78}$$

where γ_3 is another number that depends on the specific regulator choice ($\gamma_3 = \gamma_1/3$ for a sharp momentum cutoff, for example). This more severe cutoff dependence can be absorbed in a renormalization of both g_3^2 and Δ_3 and, as usual in an EFT, after renormalization the loop contributes a non-analytic term ik^3. Relative to $\tilde{T}_{1d}$, this contribution is $\mathcal{O}(\aleph/M_c)$, that is, one order down in the expansion. This means the dimeron propagator can generically be treated in perturbation theory, the LO amplitude being given by Eq. (4.77),

$$T^{(0)} \sim \frac{2\pi}{\mu_{3N} M_c}\left[1 - \mathcal{O}\left(\frac{Q^2}{\aleph^2}\right)\right]^{-1}. \tag{4.79}$$

With appropriate signs, this amplitude generates a pair of shallow poles on the real axis at $Q \sim \pm\aleph$. The NLO unitarity correction (4.78) moves these poles below the axis, but the resulting width is relative small, meaning the resonance is narrow.

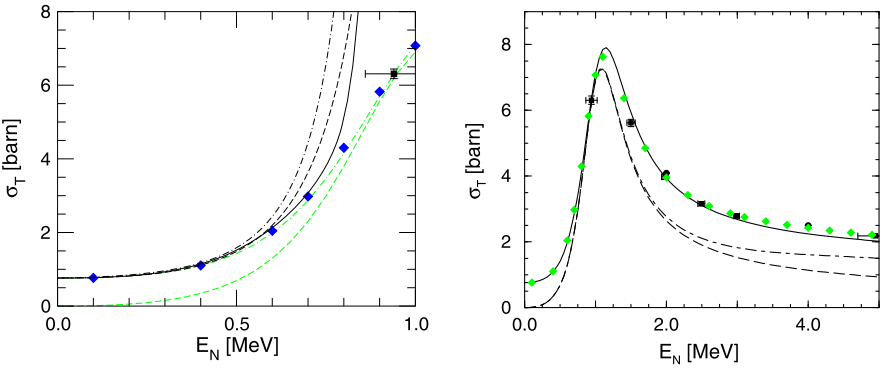

Fig. 4.11 Total cross section (in barn) for $n\alpha$ scattering as a function of the neutron kinetic energy (in MeV) in the α rest frame below (*left*) and around (*right*) the $P_{3/2}$ resonance. *Diamonds* are evaluated data [123], and *black squares* are experimental data [124, 125]. *Left*: the *dashed*, *dot–dashed* and *solid black lines* are the Halo/Cluster EFT results without resummation at LO, NLO, and N^{2}LO, and the *dashed* and *dot-dashed gray lines* the Halo/Cluster EFT results with $P_{3/2}$ resummation at LO and NLO, respectively. *Right*: the *dashed* and *solid lines* are the Halo/Cluster EFT results with $P_{3/2}$ resummation at LO and NLO, respectively. (The *dot-dashed line*, which can be ignored, shows the LO result in a modified power counting with resummation in the $P_{1/2}$ channel as well.) From Refs. [120, 122]

Now, when the external energy is in a window of $\mathcal{O}(\aleph^2/M_c)$ around the resonance the denominator in the bare propagator becomes anomalously small, requiring resummation of the propagator and bubble insertions [122] as in the S-wave bound-state case in Pionless EFT (4.73) or in the vicinity of the Delta pole in Chiral EFT:

$$\tilde{T}_{1d}+\tilde{T}_{2d}+\cdots=\frac{6\pi}{\mu_{3n}g_3^2}\left[\left(\frac{6\pi\,\Delta_3}{\mu_{3n}g_3^2}-\gamma_3\Lambda^3\right)-\left(\frac{6\pi\,\sigma_3}{2\mu_{3n}^2g_3^2}-\gamma_1\Lambda\right)k^2-ik^3\right]^{-1}\times\left[1+\mathcal{O}\left(\frac{k}{\Lambda}\right)\right], \tag{4.80}$$

which has the form of the ERE for a P wave. From this expression renormalizability is clear. It is also apparent that the scattering volume (the P-wave analog of the scattering length) is large, $\sim 1/(M_c\aleph^2)$, while the effective momentum (the P-wave analog of the effective range) is natural-sized. This leads to the characteristic bump in the cross section near the resonance energy. If the resonance is not particularly narrow a second fine-tuning is needed in the two-particle/dimeron coupling, leading to the same resummation in the whole low-energy region [120]. In this case the effective momentum is small, $\sim\aleph$. In either case, other ERE parameters come out of natural size.

A good description of $n\alpha$ scattering, displayed in Fig. 4.11, is obtained with either power counting [120, 122], the amount of fine-tuning in the ^{5}He ground state remaining unclear. When the LECs are fitted to an $n\alpha$ phase-shift analysis, one finds $M_c\sim 100$ MeV and $\aleph\sim 30$ MeV, consistent with Pionless EFT. There is in

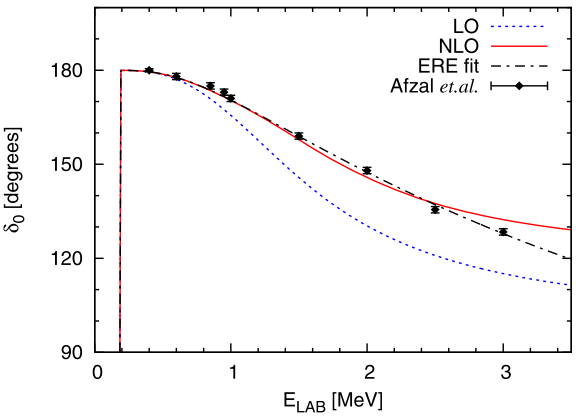

Fig. 4.12 Coulomb-corrected S-wave $\alpha\alpha$ phase shift (in degrees) as a function of the laboratory energy (in MeV). The *dotted* and *solid lines* are the Halo/Cluster EFT results at LO and NLO, respectively. *Solid circles* represent empirical phase shifts [127] and the *dash-dotted line* is an ERE fit. From Ref. [126]

principle no difficulty to include the electromagnetic interactions needed for proton halos. The extension to $p\alpha$ scattering is thus straightforward, except for a less clear separation of scales.

Coulomb is also very important for the $\alpha\alpha$ system. This system is very peculiar because the lowest resonance, with $J^\pi = 0^+$, appears at a momentum that is *small* compared to the scale Coulomb becomes important, $\alpha\mu_{\alpha\alpha}$, where $\mu_{\alpha\alpha} = m_\alpha/2$ is the $\alpha\alpha$ reduced mass. Coulomb has to be included at LO with the dimeron propagator, but it can be approximated by a $Q/\alpha\mu_{\alpha\alpha}$ expansion that makes it, in a sense, a short-range interaction. Despite its small nominal value, the resonance width is actually large in the scale set by $\aleph$. The position and width of the resonance, and the $\alpha\alpha$ phase shifts, can be well reproduced at LO and even better at NLO, as shown in Fig. 4.12 [126]. However, this is only possible only at the cost of cancellations between the short-range interaction and Coulomb at the level of factors of 100 and 10 in the scattering length and effective range, respectively. Such an additional fine-tuning is extremely surprising, and not at all understood.

External probes can be included as well. For cores for which the two-body system sustains a bound state, one can for example consider astrophysically interesting neutron-capture reactions, such as $p + {}^7\mathrm{Be} \to {}^8\mathrm{B} + \gamma$, which can be analyzed as was $p + n \to d + \gamma$ in Pionless EFT [128]. Halo/Cluster EFT offers the possibility of a controlled extrapolation of data to immeasurably small energies. For work in this direction, see Ref. [129] and references therein.

4.4.3.2 Three-Body Systems and Beyond

As for Pionless EFT, the real power of Halo/Cluster EFT lies in going beyond the ERE. For few-body systems, the question resurfaces of the relative size of few-body forces in the presence of fine-tuning, now with nucleon-core and core-core interactions that, as we have just seen, have quite a different power counting compared to the $2N$ system.

For α-core systems the two-body forces have been determined to NLO: the $N\alpha$ and $\alpha\alpha$ interactions from $N\alpha$ and $\alpha\alpha$ scattering, respectively, as described in Sect. 4.4.3.1, and the $2N$ interaction from $2N$ scattering, as described in Sect. 4.4.2.1. We can then test RG invariance without three-body forces for the three-body halo states in ^{6}He, ^{9}Be and ^{12}C, just as we did for the $p+n+n$ system [87] in Sect. 4.4.2.2. This issue has now been settled only in ^{6}He [130], ^{9}Be being under study [131].

^{6}He has been studied by adapting the Gamow Shell Model to the LO, energy-dependent interactions in the power counting of Ref. [120]. Without three-body forces, the three-body ground state collapses, while the simplest three-body force, shown explicitly in Eq. (4.75), was found sufficient for renormalization: its LEC can be adjusted to reproduce the experimental binding energy of ^{6}He at any cutoff. This three-body force is the EFT rendition of the phenomenological strategy of allowing the nn interaction to be empirically modified by the presence of the core. One can now proceed to calculate other ^{6}He properties, and more-neutron members of the He family, such as ^{8}He. Of course, one needs to check whether four-body forces are absent from LO as it seems to be the case for $p+p+n+n$ [108], as discussed in Sect. 4.4.2.3. Note that ^{6}He is Borromean, but its different nature compared to triton in Pionless EFT does not seem to diminish the importance of three-body forces.

The EFT is also a tool to look for Efimov-like states in halo nuclei. Several candidate nuclei with S-wave interactions have been studied in this fashion, giving some tantalizing hints of the answer (see Ref. [132] and references therein). Recently even the form factors of three-body S-wave halos have been calculated [133].

4.4.4 Summary

QCD exhibits in the two-nucleon system a certain amount of fine-tuning, which results in shallow bound states and resonances in light nuclei. These states can be described by EFTs with only contact interactions: Pionless EFT with only nucleon degrees of freedom, and Halo/Cluster EFT with additional degrees of freedom for tight clusters of nucleons. Good descriptions of data on S-shell nuclei and α-core halo/cluster states can be achieved, but in the case of the $\alpha\alpha$ system only at the cost of a baffling additional fine-tuning, this time between strong and electromagnetic interactions.

4.5 Conclusions and Outlook

I introduced the general concept of EFTs. Using the example of atoms in NRQED, I presented the EFTs of QCD for typical nuclei (Chiral EFT), for the lightest nuclei (Pionless EFT), and for larger nuclei with halo or cluster structure (Halo/Cluster EFT). Along the way, I alluded to some of the applications to cold-atom physics.

I described many of the successes of EFT approach, although my emphasis has been on the conceptual development. The main message is that EFT provides *the* framework to describe nuclear physics within the Standard Model (which itself can be viewed as an EFT): it is consistent with the symmetries, incorporates hadronic physics, and has a controlled expansion.

The frontier is to push EFTs in the direction of heavier nuclei. Is there a connection to the traditional Shell Model, perhaps generalizing Halo/Cluster EFT? For heavy, deformed nuclei, an EFT has been developed for the very low-energy rotational bands [134], and certainly other nuclear regimes await new EFTs. The EFT program is paving the road for a QCD understanding of nuclear structure and reactions, while uncovering some new, beautiful renormalization phenomena.

Acknowledgements I thank my many collaborators over the years for their help in shaping my views of EFTs, especially in the challenging nuclear context. This work was supported in part by the Université Paris Sud under the program "Attractivité 2013", and by the US DOE under grant DE-FG02-04ER41338.

References

1. S. Weinberg, Phys. Lett. B **251**, 288 (1990)
2. S. Weinberg, Nucl. Phys. B **363**, 3 (1991)
3. C. Ordóñez, U. van Kolck, Phys. Lett. B **291**, 459 (1992)
4. S. Weinberg, Phys. Lett. B **295**, 114 (1992)
5. T.-S. Park, D.-P. Min, M. Rho, Phys. Rep. **233**, 341 (1993)
6. U. van Kolck, Soft physics: applications of effective chiral Lagrangians to nuclear physics and quark models. Ph.D dissertation, University of Texas, 1993, UMI-94-01021
7. C. Ordóñez, L. Ray, U. van Kolck, Phys. Rev. Lett. **72**, 1982 (1994)
8. U. van Kolck, Phys. Rev. C **49**, 2932 (1994)
9. U. van Kolck, Few-Body Syst., Suppl. **9**, 444 (1995)
10. C. Ordóñez, L. Ray, U. van Kolck, Phys. Rev. C **53**, 2086 (1996)
11. U. van Kolck, Prog. Part. Nucl. Phys. **43**, 337 (1999)
12. S.R. Beane, P.F. Bedaque, W.C. Haxton, D.R. Phillips, M.J. Savage, nucl-th/0008064
13. P.F. Bedaque, U. van Kolck, Annu. Rev. Nucl. Part. Sci. **52**, 339 (2002)
14. E. Epelbaum, H.-W. Hammer, U.-G. Meißner, Rev. Mod. Phys. **81**, 1773 (2009)
15. H.-W. Hammer, L. Platter, Annu. Rev. Nucl. Part. Sci. **60**, 207 (2010)
16. R. Machleidt, D.R. Entem, Phys. Rep. **503**, 1 (2011)
17. J. Beringer et al. (Particle Data Group), Phys. Rev. D **86**, 010001 (2012)
18. S. Weinberg, Phys. A **96**, 327 (1979)
19. G.P. Lepage, hep-ph/0506330
20. J. Polchinski, hep-th/9210046
21. D.B. Kaplan, nucl-th/9506035
22. U. van Kolck, L.J. Abu-Raddad, D.M. Cardamone, nucl-th/0205058
23. G. 't Hooft, NATO Adv. Stud. Inst. Ser. B Phys. **59**, 135 (1980)
24. S. Weinberg, *The Quantum Theory of Fields, Vol. 1: Foundations* (Cambridge University Press, Cambridge, 1995)
25. A. Manohar, H. Georgi, Nucl. Phys. B **234**, 189 (1984)
26. H. Georgi, L. Randall, Nucl. Phys. B **276**, 241 (1986)
27. T.Y. Cao, in *Renormalization. From Lorentz to Landau (and beyond)*, ed. by L.M. Brown (Springer, Berlin, 1993), pp. 87–133

28. S. Hartmann, Stud. Hist. Philos. Mod. Phys. **32**, 267 (2001)
29. W.E. Caswell, G.P. Lepage, Phys. Lett. B **167**, 437 (1986)
30. H. Georgi, Phys. Lett. B **240**, 447 (1990)
31. T. Mannel, W. Roberts, Z. Ryzak, Nucl. Phys. B **368**, 204 (1992)
32. D.A. Dicus, C. Kao, W.W. Repko, Phys. Rev. D **57**, 2443 (1998)
33. M.E. Luke, A.V. Manohar, Phys. Lett. B **286**, 348 (1992)
34. R.J. Hill, G. Lee, G. Paz, M.P. Solon, Phys. Rev. D **87**, 053017 (2013)
35. B.R. Holstein, Am. J. Phys. **72**, 333 (2004)
36. P. Labelle, S.M. Zebarjad, C.P. Burgess, Phys. Rev. D **56**, 8053 (1997)
37. U.D. Jentschura, A. Czarnecki, K. Pachucki, Phys. Rev. A **72**, 062102 (2005)
38. E. Mereghetti, W.H. Hockings, U. van Kolck, Ann. Phys. **325**, 2363 (2010)
39. S. Weinberg, *The Quantum Theory of Fields, Vol. 2: Modern Applications* (Cambridge University Press, Cambridge, 1996)
40. S. Weinberg, Trans. N. Y. Acad. Sci. **38**, 185 (1977)
41. V. Baluni, Phys. Rev. D **19**, 2227 (1979)
42. C.A. Baker et al., Phys. Rev. Lett. **97**, 131801 (2006)
43. D.B. Kaplan, M.J. Savage, Nucl. Phys. A **556**, 653 (1993). [Erratum-ibid. A **570**, 833 (1994)] [Erratum-ibid. A **580**, 679 (1994)]
44. S.-L. Zhu, C.M. Maekawa, B.R. Holstein, M.J. Ramsey-Musolf, U. van Kolck, Nucl. Phys. A **748**, 435 (2005)
45. J. de Vries, E. Mereghetti, R.G.E. Timmermans, U. van Kolck, Ann. Phys. **338**, 50 (2013)
46. S. Scherer, M.R. Schindler, hep-ph/0505265
47. B. Long, U. van Kolck, Nucl. Phys. A **840**, 39 (2010)
48. B. Long, U. van Kolck, Nucl. Phys. A **870–871**, 72 (2011)
49. V. Bernard, N. Kaiser, U.-G. Meißner, Int. J. Mod. Phys. E **4**, 193 (1995)
50. V. Pascalutsa, D.R. Phillips, Phys. Rev. C **67**, 055202 (2003)
51. V. Bernard, Prog. Part. Nucl. Phys. **60**, 82 (2008)
52. J.L. Friar, Phys. Rev. C **60**, 034002 (1999)
53. N. Kaiser, R. Brockmann, W. Weise, Nucl. Phys. A **625**, 758 (1997)
54. N. Kaiser, S. Gerstendorfer, W. Weise, Nucl. Phys. A **637**, 395 (1998)
55. M.C.M. Rentmeester, R.G.E. Timmermans, J.L. Friar, J.J. de Swart, Phys. Rev. Lett. **82**, 4992 (1999)
56. M.C.M. Rentmeester, R.G.E. Timmermans, J.J. de Swart, Phys. Rev. C **67**, 044001 (2003)
57. N. Kaiser, Phys. Rev. C **65**, 017001 (2002)
58. J.L. Friar, D. Hüber, U. van Kolck, Phys. Rev. C **59**, 53 (1999)
59. D. Hüber, J.L. Friar, A. Nogga, H. Witała, U. van Kolck, Few-Body Syst. **30**, 95 (2001)
60. E. Epelbaum, Phys. Lett. B **639**, 456 (2006)
61. E. Epelbaum, Eur. Phys. J. A **34**, 197 (2007)
62. J.L. Friar, G.L. Payne, U. van Kolck, Phys. Rev. C **71**, 024003 (2005)
63. E. Epelbaum, A. Nogga, W. Glöckle, H. Kamada, U.-G. Meißner, H. Witała, Phys. Rev. C **66**, 064001 (2002)
64. H.-W. Hammer, A. Nogga, A. Schwenk, Rev. Mod. Phys. **85**, 197 (2013)
65. S.R. Beane, V. Bernard, T.S.H. Lee, U.-G. Meißner, U. van Kolck, Nucl. Phys. A **618**, 381 (1997)
66. U. van Kolck, J.A. Niskanen, G.A. Miller, Phys. Lett. B **493**, 65 (2000)
67. S.R. Beane, P.F. Bedaque, M.J. Savage, U. van Kolck, Nucl. Phys. A **700**, 377 (2002)
68. D.B. Kaplan, M.J. Savage, M.B. Wise, Nucl. Phys. B **478**, 629 (1996)
69. D.B. Kaplan, M.J. Savage, M.B. Wise, Nucl. Phys. B **534**, 329 (1998)
70. S. Fleming, T. Mehen, I.W. Stewart, Nucl. Phys. A **677**, 313 (2000)
71. S.R. Beane, P.F. Bedaque, L. Childress, A. Kryjevski, J. McGuire, U. van Kolck, Phys. Rev. A **64**, 042103 (2001)
72. A. Nogga, R.G.E. Timmermans, U. van Kolck, Phys. Rev. C **72**, 054006 (2005)
73. M.C. Birse, Phys. Rev. C **74**, 014003 (2006)
74. B. Long, U. van Kolck, Ann. Phys. **323**, 1304 (2008)

75. M.C. Birse, Philos. Trans. R. Soc. Lond. A **369**, 2662 (2011)
76. C.-J. Yang, C. Elster, D.R. Phillips, Phys. Rev. C **80**, 034002 (2009)
77. Ch. Zeoli, R. Machleidt, D.R. Entem, arXiv:1208.2657 [nucl-th]
78. E. Epelbaum, U.-G. Meißner, nucl-th/0609037
79. M. Pavón Valderrama, Phys. Rev. C **83**, 024003 (2011)
80. B. Long, C.-J. Yang, Phys. Rev. C **84**, 057001 (2011)
81. M. Pavón Valderrama, Phys. Rev. C **84**, 064002 (2011)
82. B. Long, C.-J. Yang, Phys. Rev. C **85**, 034002 (2012)
83. B. Long, C.-J. Yang, Phys. Rev. C **86**, 024001 (2012)
84. S.R. Beane, P.F. Bedaque, K. Orginos, M.J. Savage, Phys. Rev. Lett. **97**, 012001 (2006)
85. S.R. Beane, E. Chang et al., Phys. Rev. C **88**, 024003 (2013)
86. D.B. Kaplan, Nucl. Phys. B **494**, 471 (1997)
87. P.F. Bedaque, H.-W. Hammer, U. van Kolck, Nucl. Phys. A **676**, 357 (2000)
88. P.F. Bedaque, U. van Kolck, Phys. Lett. B **428**, 221 (1998)
89. U. van Kolck, Nucl. Phys. A **645**, 273 (1999)
90. S.R. Beane, T.D. Cohen, D.R. Phillips, Nucl. Phys. A **632**, 445 (1998)
91. X. Kong, F. Ravndal, Nucl. Phys. A **665**, 137 (2000)
92. J.-W. Chen, G. Rupak, M.J. Savage, Nucl. Phys. A **653**, 386 (1999)
93. E. Braaten, H.-W. Hammer, Phys. Rep. **428**, 259 (2006)
94. V.G.J. Stoks, R.A.M. Klomp, M.C.M. Rentmeester, J.J. de Swart, Phys. Rev. C **48**, 792 (1993)
95. P.F. Bedaque, H.-W. Hammer, U. van Kolck, Phys. Rev. C **58**, 641 (1998)
96. P.F. Bedaque, H.-W. Hammer, U. van Kolck, Phys. Rev. Lett. **82**, 463 (1999)
97. P.F. Bedaque, H.-W. Hammer, U. van Kolck, Nucl. Phys. A **646**, 444 (1999)
98. P.F. Bedaque, G. Rupak, H.W. Grießhammer, H.-W. Hammer, Nucl. Phys. A **714**, 589 (2003)
99. W. Dilg, L. Koester, W. Nistler, Phys. Lett. B **36**, 208 (1971)
100. W.T.H. van Oers, J.D. Seagrave, Phys. Lett. B **24**, 562 (1967)
101. A.C. Phillips, G. Barton, Phys. Lett. B **28**, 378 (1969)
102. A. Kievsky, S. Rosati, W. Tornow, M. Viviani, Nucl. Phys. A **607**, 402 (1996)
103. L. Platter, Phys. Rev. C **74**, 037001 (2006)
104. S. Koenig, H.-W. Hammer, Phys. Rev. C **83**, 064001 (2011)
105. L. Platter, H.-W. Hammer, Nucl. Phys. A **766**, 132 (2006)
106. C. Ji, D.R. Phillips, L. Platter, Ann. Phys. **327**, 1803 (2012)
107. L. Platter, H.-W. Hammer, U.-G. Meißner, Phys. Rev. A **70**, 052101 (2004)
108. L. Platter, H.-W. Hammer, U.-G. Meißner, Phys. Lett. B **607**, 254 (2005)
109. J. Kirscher, H.W. Grießhammer, D. Shukla, H.M. Hofmann, Eur. Phys. J. A **44**, 239 (2010)
110. T. Mehen, I.W. Stewart, M.B. Wise, Phys. Rev. Lett. **83**, 931 (1999)
111. H.M. Müller, S.E. Koonin, R. Seki, U. van Kolck, Phys. Rev. C **61**, 044320 (2000)
112. I. Stetcu, B.R. Barrett, U. van Kolck, Phys. Lett. B **653**, 358 (2007)
113. S.R. Beane, P.F. Bedaque, A. Parreño, M.J. Savage, Phys. Lett. B **585**, 106 (2004)
114. I. Stetcu, J. Rotureau, B.R. Barrett, U. van Kolck, Ann. Phys. **325**, 1644 (2010)
115. J. Rotureau, I. Stetcu, B.R. Barrett, M.C. Birse, U. van Kolck, Phys. Rev. A **82**, 032711 (2010)
116. D. Lee, Prog. Part. Nucl. Phys. **63**, 117 (2009)
117. I. Stetcu, J. Rotureau, Prog. Part. Nucl. Phys. **69**, 182 (2013)
118. S.A. Coon, M.I. Avetian, M.K.G. Kruse, U. van Kolck, P. Maris, J.P. Vary, Phys. Rev. C **86**, 054002 (2012)
119. S.N. More, A. Ekstrom, R.J. Furnstahl, G. Hagen, T. Papenbrock, Phys. Rev. C **87**, 044326 (2013)
120. C.A. Bertulani, H.-W. Hammer, U. van Kolck, Nucl. Phys. A **712**, 37 (2002)
121. TUNL Nuclear Data Evaluation Project, http://www.tunl.duke.edu/nucldata/
122. P.F. Bedaque, H.-W. Hammer, U. van Kolck, Phys. Lett. B **569**, 159 (2003)
123. National Nuclear Data Center Evaluated Nuclear Data Files, Brookhaven National Laboratory, http://www.nndc.bnl.gov/

124. B. Haesner et al., Phys. Rev. C **28**, 995 (1983)
125. M.E. Battat et al., Nucl. Phys. **12**, 291 (1959)
126. R. Higa, H.-W. Hammer, U. van Kolck, Nucl. Phys. A **809**, 171 (2008)
127. S.A. Afzal, A.A.Z. Ahmad, S. Ali, Rev. Mod. Phys. **41**, 247 (1969)
128. G. Rupak, Nucl. Phys. A **678**, 405 (2000)
129. G. Rupak, R. Higa, Phys. Rev. Lett. **106**, 222501 (2011)
130. J. Rotureau, U. van Kolck, Few-Body Syst. **54**, 725 (2013)
131. S. Ando et al., in progress
132. B. Acharya, C. Ji, D.R. Phillips, Phys. Lett. B **723**, 196 (2013)
133. P. Hagen, H.-W. Hammer, L. Platter, Eur. Phys. J. A **49**, 118 (2013)
134. T. Papenbrock, Nucl. Phys. A **852**, 36 (2011)